Designing polymers for advanced battery chemistries

Jeffrey Lopez [ID][1], David G. Mackanic [ID][1], Yi Cui [ID][2,3] and Zhenan Bao [ID][1] *

Abstract | Electrochemical energy storage devices are becoming increasingly important to our global society, and polymer materials are key components of these devices. As the demand for high-energy density devices increases, innovative new materials that build on the fundamental understanding of physical phenomena and structure–property relationships will be required to enable high-capacity next-generation battery chemistries. In this Review, we discuss core polymer science principles that are used to facilitate progress in battery materials development. Specifically, we discuss the design of polymeric materials for desired mechanical properties, increased ionic and electronic conductivity and specific chemical interactions. We also discuss how polymer materials have been designed to create stable artificial interfaces and improve battery safety. The focus is on these design principles applied to advanced silicon, lithium-metal and sulfur battery chemistries.

The development of new electrochemical energy storage technologies has been instrumental to the proliferation of portable electronic devices and the increasing adoption of electric vehicles. Intermittent electricity generation (for example, from wind and solar power sources) has further intensified the demand for high-energy density, high-power and low-cost energy storage devices[1,2]. Polymer materials are ubiquitous in these energy storage devices and are commonly used as binders, electrolytes, separators and package coatings to provide structural support, adhesion and mechanical stability to the devices (FIG. 1; TABLE 1). Separators with pore sizes of ~30–100 nm are commonly made from uniaxially stretched polyethylene or polypropylene and serve to electrically isolate the two electrodes while providing ionic conduction pathways through the liquid electrolyte that fills the pores[3] (FIG. 1c). Polymers are also used as binders to increase the cohesion of particles in the composite electrodes and their adhesion to the metal current collector[4] (FIG. 1b). The binder also increases the viscosity of the electrode slurry to ensure high-quality (that is, uniform and smooth) coating of the slurry onto the current collector. The scale at which batteries are being manufactured is growing quickly, and thus the cost and processability of devices are key considerations. For commercial application in energy storage devices, new polymer materials should ideally be easy to synthesize from inexpensive reagents and processable in environmentally friendly and non-toxic solvents.

As the demand for higher performance batteries grows, researchers are turning to new polymers with advanced functionalities to help improve the operation of existing materials or to enable the application of new battery chemistries. In this Review, we summarize the fundamental polymer science and engineering concepts related to the development of polymers for next-generation battery applications (TABLE 1). We specifically discuss how these core concepts drive the design of new polymer materials for advanced battery chemistries, including Si, Li-metal and S electrodes.

Advanced battery chemistries

Si anodes. Si has a high theoretical specific capacity of 3,579 mAh g^{-1} for Li$_{3.6}$Si and has the potential to replace graphite (372 mAh g^{-1}) as the negative-electrode active material in Li-ion batteries[5,6]. Although Panasonic has already begun to incorporate Si into their graphite anodes[7,8], the large volume expansion (~300%) of Si during lithiation has prevented its utilization as a majority component of the active materials[6,9,10]. As Si expands, large anisotropic stresses build up that cause the particles to fracture and the capacity to quickly fade[9,11,12] (FIG. 2a). The failure of Si electrodes results from two mechanisms. First, cracks in the Si particles provide fresh surfaces for electrolyte decomposition reactions and solid electrolyte interphase (SEI) formation[13,14], and second, portions of Si can also become electrically disconnected from the rest of the electrode, which prevents further cycling[15]. Si nanoparticles circumvent these issues because fracture does not occur below a critical particle size of 150 nm (REF.[12]), and many successful materials have been developed based on this approach[16–18]. However, nanosized Si can be 1–2 orders of magnitude more expensive than larger micrometre-sized particles. Unfortunately,

[1]Department of Chemical Engineering, Stanford University, Stanford, CA, USA.

[2]Department of Materials Science and Engineering, Stanford University, Stanford, CA, USA.

[3]Stanford Institute for Materials and Energy Sciences, SLAC National Accelerator Laboratory, Menlo Park, CA, USA.
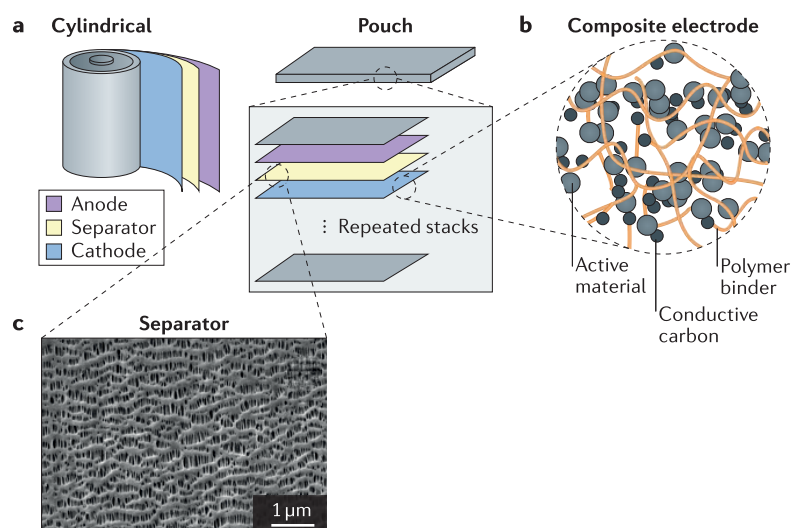
*e-mail: zbao@stanford.edu

Fig. 1 | **Polymers in commercial Li-ion batteries. a** | A cylindrical cell and pouch cell with rolled and stacked configurations, respectively. **b** | Illustration of a composite electrode containing a polymer binder, active material and conductive additive. **c** | Scanning electron microscopy image of a porous polymer separator. Panel **c** is adapted with permission from REF.[3], American Chemical Society.

serious particle fracture and rapid failure prevent the effective use of micrometre-sized Si (REFS[12,19,20]). To successfully enable the use of larger Si particles or to further improve the performance of nanosized Si, researchers have turned to encapsulating the Si particles in protective carbon shells[21] or modifying the polymer binder used in the composite electrode[22–24]. The polymer-based approach is discussed further below from the perspective of mechanical properties, electronic conductivity and binding interactions.

Li-metal anodes. Beyond Si, Li metal offers the highest theoretical energy density owing to its low potential (−3.04 V versus the standard hydrogen electron) and high capacity (3,860 mAh g^{-1})[25], but successful application has eluded researchers for more than four decades owing to poor Coulombic efficiency and safety issues[7]. A key challenge for ensuring safe and efficient Li-metal electrodes is the formation of a stable, uniform SEI layer on the Li surface that can withstand the large volumetric change during cycling[26–28]. Local variations in the composition of the SEI layer can lead to non-uniform deposition of Li owing to changes in Li-ion conductivity across the electrode or breakage of the SEI. These SEI defects facilitate the growth of high-surface-area Li dendrites that increase electrolyte decomposition and cause the accumulation of dead Li, which leads to increased impedance and capacity loss[29] (FIG. 2b). The resulting dendrites can also eventually grow through the battery separator and cause short circuiting and thermal runaway[30,31]. Approaches to solve these issues include modifying the concentration of the salt in the liquid electrolyte[32–35], increasing the fluorine content in the electrolyte[36,37] or using additives for improved Li deposition[38–40]. Here, we focus on the use of polymer materials as electrolytes or coatings to suppress dendrite growth and improve safety.

S cathodes. For the positive electrode, Li-metal oxides (LiM$_x$O, M = Co, Ni or Mn) or phosphates (for example, LiFePO$_4$) are currently used, but the capacity of these materials is limited[7]. Sulfur offers a promising alternative with a high capacity of ~1,700 mAh g^{-1} for Li$_2$S, which is approximately seven times higher than the capacity of the metal oxides (~250 mAh g^{-1})[41]. Unfortunately, the intermediate lithium polysulfide species that form as S is reduced are soluble in the liquid organic electrolytes[42] (FIG. 2c). These soluble species eventually migrate to and deposit on the anode. This self-discharge reduces the capacity of the cell but also contributes to the build-up of an insulating layer on top of the anode that limits cycling stability. Moreover, the S electrodes have poor electronic conductivity and thus require large amounts of conductive carbon to function, which reduces the energy density[43]. Efforts to prevent polysulfide dissolution have focused on the development of functional cathodes that can chemically bind the polysulfide species. Nitrogen-doped carbon materials have been some of the most successful in this regard because of their high electronic conductivity and polysulfide-binding ability[42]. Additionally, nanostructuring of the cathode can help to prevent polysulfide dissolution by physically trapping the species[44]. We discuss below polymer materials that are used to increase the conductivity of the composite electrode or to trap polysulfide species.

Overall, new battery chemistries offer promising paths towards high-performance energy storage (FIG. 2d) for improved sustainability, and there is a significant opportunity for innovation in polymer science and engineering to help solve longstanding problems and enable the development of these devices. This Review serves as an introduction to the fundamental materials requirements for advanced battery chemistries and the central concepts related to polymer design for these applications. Owing to the breadth of topics covered, we focus only on central works that are directly related to the design of polymers for advanced battery chemistries.

Designing binder and separator mechanics

Polymer mechanics. Perhaps some of the most familiar aspects of polymer materials are their mechanical properties. The main method used to analyse the mechanical properties of a polymer is the stress–strain curve (FIG. 3a). As strain is applied to a polymer, the stress increases linearly at first, but as the strain continues to increase, the material may continue to stretch elastically (no slope change), begin to yield (a reduction in slope) or break. Materials that yield undergo irreversible plastic deformation, which typically involves the molecular rearrangement of the polymer chains via sliding or rotation.

Several metrics can be used to quantify the mechanical properties of polymer materials, including the modulus, tensile strength, elongation to break, toughness and resilience[45,46]. The initial slope of the stress–strain curve is used to calculate Young's modulus, which is one of the most commonly discussed parameters. The modulus describes how rigid a material is but does not describe the strength or durability of the material. Tensile strength refers to the stress required to break the material and is taken from the maximum stress on the stress–strain

Table 1 | **Summary of polymer materials used to enable advanced battery chemistries**

Application	Challenges	Solutions	Representative polymer materials
Si-anode binders	• Particle pulverization • Electrical isolation of active materials • Build-up of SEI	• Hydrogen bonding with Si surface[23,66,67] • Increased binder elasticity[24] • Electrolyte swelling for higher rate[135,139,172] • Added electronic conductivity[133,134,174]	• Crosslinked poly(acrylic acid) • Carbohydrates • Poly(3,4-ethylenedioxy thiophene) • Polyfluorene
Electrolytes and coatings for Li metal	• Growth of dendrites • Build-up of dead Li • High reactivity	• Polymer coatings to control Li deposition[81–83,187–193] • Electrolyte-modified interface to prevent dendrite growth[74–77] • High-modulus electrolytes to suppress dendrites[70–73]	• Poly(dimethylsiloxane) • Poly(vinylidene fluoride) • Lithiated Nafion • Modified poly(ethylene oxide)
S-cathode binders	• Dissolution of polysulfides • Self-discharge • Charge shuttling	• N, S and O motifs for polysulfide trapping[151–153] • Ionic polysulfide traps[156–159] • Added electronic conductivity[142–144,146]	• Poly(vinyl pyrrolidone) • Poly(aniline) • Poly(pyrrole) • Poly(3,4-ethylenedioxy thiophene)
Polymer electrolytes	• Low ionic conductivity • Low transference number	• Low T_g to increase segmental motion[88,103,105,115] • Weak cation coordination to increase cation diffusivity[111,114,116] • Anion binding to increase transference number[71]	• Modified poly(ethylene oxide) • Other polyethers • Polycarbonate or polyester
Safety	Thermal runaway	• Melting separators for cell shutdown[3] • PTC resistors for cell shutdown[201] • Flame retardants[117,205,206]	• Poly(ethylene) • Poly(propylene) • Fluoropolymers

PTC, positive thermal expansion coefficient; SEI, solid electrolyte interphase; T_g, glass transition temperature.

curve. Yield strength is similar to the tensile strength but describes the stress required to begin to plastically deform the material. The toughness of a polymer is obtained by integrating the area under the stress–strain curve and describes the amount of energy needed to break the material. Soft materials with a longer elongation to break can have a much greater toughness than hard materials with a high modulus. The modulus of resilience is similar to the toughness but does not include the contribution from plastic deformation. Resilience quantifies the energy that is reversibly stored in the material and includes only the area under the stress–strain curve before the yield point. In brief, the modulus describes how a material will respond initially to strain, strength refers to the amount of stress required to deform or break the material and toughness or resilience refers to the amount of energy required to break or deform the material.

These bulk mechanical properties arise from the molecular characteristics of the polymer chains[45]. Generally, values for the modulus, tensile strength and elongation to break increase with increasing molecular weight of the polymer. Branching or monomer structures that reduce crystallinity will decrease these mechanical properties. Crosslinking of the polymer chains to form a network structure can also be used to increase the mechanical stability of a material (FIG. 3b). If the bonding used to crosslink this network structure is dynamic, polymer systems can assume self-healing properties. When a self-healing polymer is fractured, dynamic crosslinks, such as hydrogen bonds[22], metal–ligand interactions[47,48] or reversible covalent bonds[49], break at the fracture site. Upon bringing the fractured interface back into contact, the broken bonds reform across the interface and heal the material. Furthermore, owing to

the high molecular weight and range of relaxation times present in polymer materials, the mechanical properties of polymers are often highly dependent on the timescale and temperature of the measurement. Measurements of the shear modulus (FIG. 3c) show that, over long timescales (low frequencies), some polymer materials can flow like liquids, whereas at short timescales, they behave like solids. This nonlinear viscoelastic behaviour is discussed only briefly below but is important to consider when designing polymers.

Elastic and self-healing binders to prolong Si cycle life. The use of Si as a high-capacity negative-electrode material is limited by its large volume expansion upon lithiation[6,9,10] and the resulting fracture of the particles and destruction of the composite electrode[9,11,12]. Poly(vinylidene fluoride) (PVDF) is traditionally used as a binder for composite electrodes, but its brittle nature and poor adhesion to Si particles have prompted the search for alternative materials[15,50] (FIG. 3d). Below, we discuss binders with mechanical properties that have been engineered for improved cycling stability.

There is a large body of work focused on novel binders for Si, and readers are directed to other reviews for a more comprehensive overview of the area[4,51–53]. Although a binder with suitable mechanical properties is crucial to achieving stable cycling, a binder with a high modulus is not enough to prevent capacity fade. For example, although polyimide typically has a modulus >1 GPa, when used as a binder for Si electrodes, 80% of the initial capacity is maintained for only 20 cycles[54]. Ideally, a binder should have strong adhesion to the active material, carbon additive and current collector while also exhibiting good electrochemical stability and high ionic conductivity. In addition, the ideal binder for
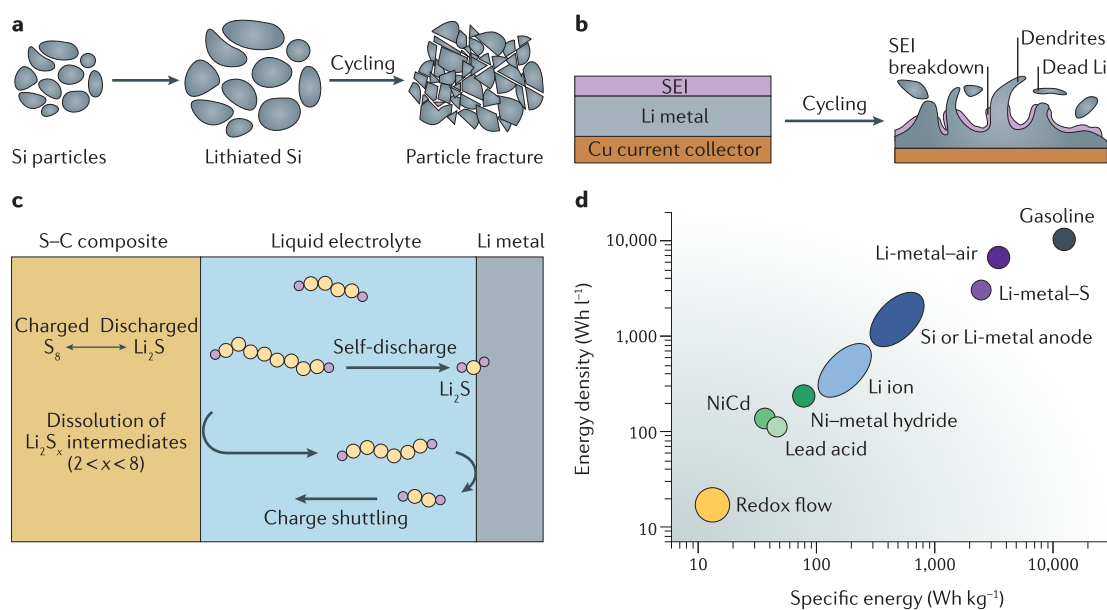
Fig. 2 | **Advanced battery chemistries and related challenges. a** | Repeated lithiation causes the pulverization of Si particles. **b** | The formation of defects in the solid electrolyte interphase (SEI) can facilitate the growth of Li dendrites and accumulation of dead Li during cycling. **c** | Dissolution of polysulfide species from the S cathode results in self-discharge and charge shuttling. Self-discharge occurs when oxidized Li_2S_x species diffuse to the Li-metal anode and are reduced during discharge or storage, decreasing the usable capacity of the cell. The reduction of oxidized Li_2S_x species at the anode during charging is known as charge shuttling and leads to a low Coulombic efficiency, as a single S atom is oxidized multiple times as charge is passed across the cell through the electrolyte. **d** | The energy density and specific energy of advanced battery chemistries (Si, Li metal and S) are compared with those of commercial battery chemistries (lead acid, NiCd, Ni–metal hydride and Li-ion based on graphite anodes and metal oxide cathodes).

Si should be able to maintain the integrity of the composite electrode during the large volume changes that occur. To this end, two different approaches have been taken: the first focuses on creating elastic binders that can reversibly compensate for the strain in the electrode, and the second focuses on creating binders with dynamic bonding to continually adapt to the changing mechanical environment during cycling.

The design of elastomeric materials is straightforward. Conceptually, a network must be created with nodes that 'remember' their position such that deformed polymer chains can relax back to their original states after the strain is released[55] (FIG. 3b). Typically, crosslinking is accomplished by using hard segments, such as styrene in styrene–butadiene rubber and diphenyl groups (for example, methylene diphenyl diisocyanate) in polyurethane, that phase separate from the soft segments, which can easily stretch. Alternatively, monomers that form a branching point during polymerization or contain reactive side chains for post-polymerization crosslinking are used to create a polymer mesh in which a network structure is fixed through covalent bonding.

Early approaches to creating elastomeric binders used crosslinked PVDF[56] or the addition of elastic styrene–butadiene rubber to a carbohydrate binder mixture[57]. Unfortunately, these approaches were relatively unsuccessful owing to the non-interacting nature of PVDF and styrene–butadiene rubber with Si particles. Carbohydrate and other hydroxyl-containing polymers were identified as superior binders[58–60], and crosslinking of these materials was used to further improve cycling

stability. In situ thermal crosslinking of poly(acrylic acid) (PAA)-based binders with the alcohol functional groups of carboxymethyl cellulose (CMC)[61] or poly(vinyl alcohol)[62] was used to form a network structure within the composite electrode that also included bonding to the hydroxyl-terminated Si surface (FIG. 3d). Radical polymerization has also been used to develop electrodes based on crosslinked CMC–PAA[63] and polyacrylamide[64].

In addition to covalent crosslinks, noncovalent metal-ion crosslinking[47,48], hydrogen bonding[22] and host–guest interactions[65] (FIG. 3d) have been used to enable longer cycling lifetimes of Si electrodes. These supramolecular interactions allow for a different kind of reversibility to that exhibited by elastomers, as they can rearrange and heal fractures that occur in the electrode composite. A systematic study found that materials with these supramolecular interactions perform better than their covalently crosslinked counterparts[66], and a self-healing binder based on hydrogen bonding was the first to successfully enable long cycling with large Si particles at commercially relevant mass loadings[23]. Recently, elastic crosslinked binders based on modified PAA have also shown stable cycling at high mass loadings[24,67].

Rheological studies of a supramolecular binder indicate that it is possible to optimize the material by fine-tuning the mechanical properties through variations in the crosslinking density of the network; however, this optimization is ultimately a secondary effect to the functional groups present in the binder[68]. Upon examining demonstrations of high areal capacity and long cycling stability using micrometre-sized Si particles, modified PAA
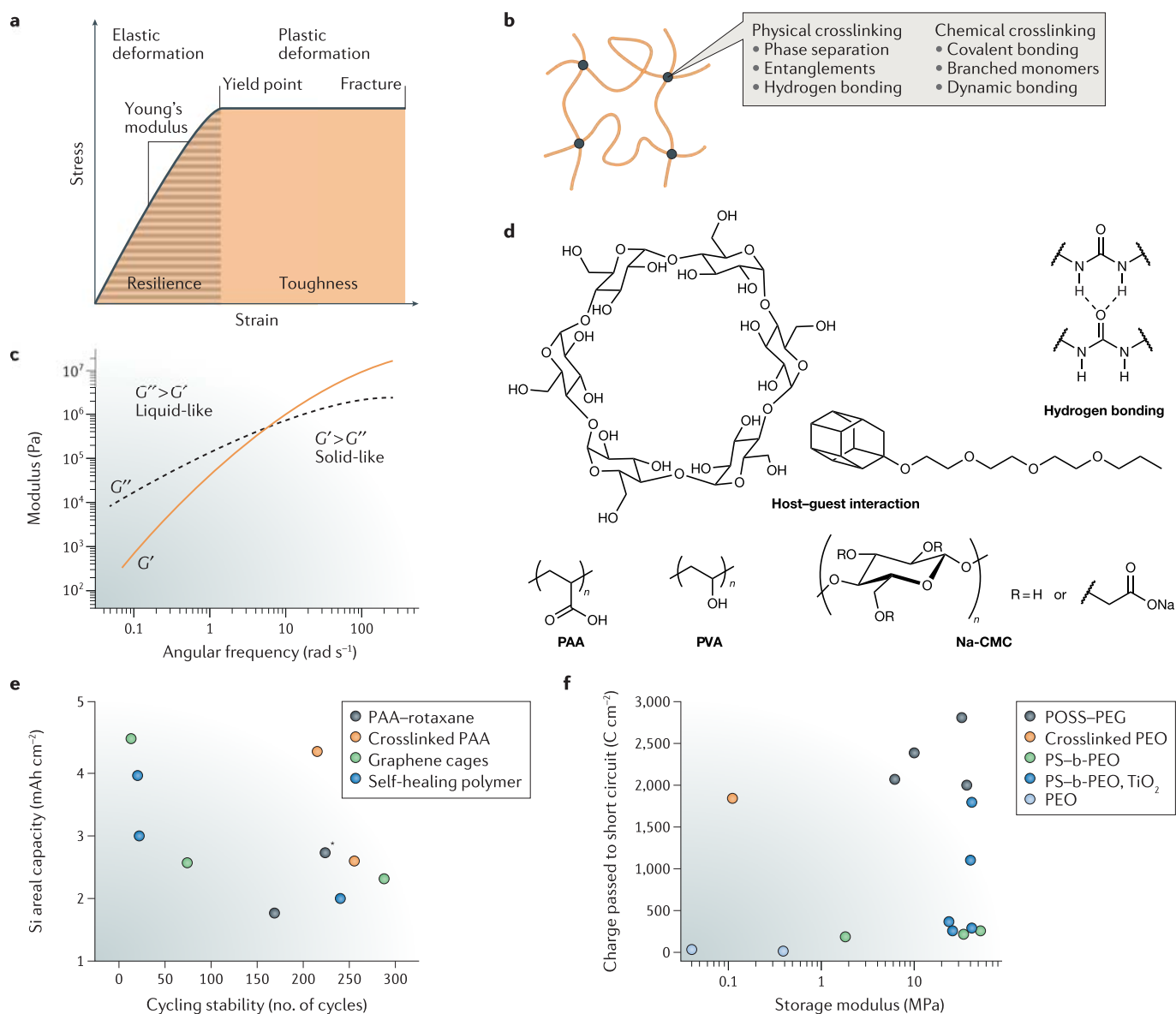
a

b

Physical crosslinking	Chemical crosslinking
• Phase separation	• Covalent bonding
• Entanglements	• Branched monomers
• Hydrogen bonding	• Dynamic bonding

c

d

Hydrogen bonding

Host–guest interaction

PAA   PVA   Na-CMC   R = H   or

e

f

Fig. 3 | **Mechanical properties of polymers. a** | A stress–strain curve for typical polymers with various features indicated. **b** | A network diagram of a crosslinked polymer with the crosslinking nodes shown as filled circles. **c** | A frequency sweep showing the crossover region for a viscoelastic material and illustrating the time dependence of polymer mechanical properties. **d** | The chemical structures of supramolecular bonding groups and Si binders (poly(acrylic acid) (PAA), poly(vinyl alcohol) (PVA) and sodium carboxymethylcellulose (Na-CMC)). **e** | Plot of the areal capacity versus the number of cycles at which the cell reached 85% of its capacity after formation cycles. Data are reported for electrodes using large micrometre-sized Si particles and different binders: a PAA–rotaxane[24] (*extrapolation from reported data; 90% capacity retention reported at 150 cycles), crosslinked PAA[67] and a self-healing polymer[23]. The performance of these systems is compared with that of Si particles coated in graphene cages[21]. **f** | Li dendrites can be mechanically suppressed with a high-modulus polymer electrolyte. Electrolytes with a higher modulus enable more total charge to pass during symmetric cell cycling before short circuit. Data are shown for polyhedral oligomeric silsesquioxane (POSS)–poly(ethylene glycol) (PEG)[77], crosslinked poly(ethylene oxide) (PEO)[75], polystyrene–block-PEO (PS–b-PEO)[70], PS–b-PEO with a TiO$_2$ filler (PS–b-PEO, TiO$_2$)[72] and PEO[70,75]. Values measured with a current density between 0.17 mA cm^{-2} and 0.30 mA cm^{-2} at 90 °C. G', shear storage modulus; G'', shear loss modulus.

binders[24,67] and a self-healing polymer binder[23] were shown to have comparable results to Si particles protected with a graphene cage[21] (FIG. 3e). These three state-of-the-art polymer binders all contain network structures and dynamic bonding groups capable of both interchain interactions and binding with the Si surface. These properties may be key to enabling the stable cycling of high-capacity Si anodes[53].

High-modulus polymers to control Li-metal dendrites.
The formation of Li-metal dendrites during operation has long prevented the application of Li-metal anodes[7,25]. In 2005, Newman and Monroe predicted[69] that an electrolyte with a shear modulus of 6 GPa could suppress dendrite propagation, which motivated the pursuit of solid electrolytes with high shear moduli to mechanically

prevent penetration by Li dendrites after their forma-tion (FIG. 3f). Unfortunately, poly(ethylene oxide) (PEO), which is the dominant matrix material for polymer elec-trolytes, has a shear modulus of, at most, 200 MPa. Rigid, well-oriented polymers have moduli well above the req-uisite value, but the chain rigidity prevents ion conduc-tion through the material. To circumvent this trade-off, block copolymers that combine a hard polystyrene block with an ion-conducting PEO block have been developed to balance mechanical properties with ionic conductiv-ity[70-72] (FIG. 3f). Hard polymers can also be blended with PEO to create high-modulus electrolytes[73], but none of these approaches has achieved room-temperature ionic conductivity above 10^{-5} S cm^{-1}.

Over the past few years, there has been debate as to the necessity of a separator with a high modulus for dendrite suppression, and low-modulus, crosslinked systems have been reported to suppress dendrites more effectively than commercial separators[74-77] (FIG. 3f). Newman and Monroe's analysis has been extended, and this updated theory suggests that the combination of increased surface tension at the metal–electrolyte inter-face and a polymer with a moderate modulus is sufficient to suppress dendrite growth when a small portion of ani-ons are immobilized in the separator[78]. This extended analysis shows that pressure induced by perturbations in Li deposition also induces ion flux away from the grow-ing dendrite tips. In a subsequent study of a crosslinked poly(propylene oxide) gel electrolyte, this linear stability analysis was used to relate the typical dendrite size (based on the most unstable perturbation wavelengths) to the pore size in the gel electrolyte and shows that smaller pores lead to denser Li deposits, as surface tension effects can suppress dendrite growth on small length scales[79]. These results indicate that, in general, high-transference polymer electrolytes, or materials with increased surface tension, could suppress dendrite growth through a mech-anism other than mechanical suppression. Indeed, many of the most successful approaches to enabling Li-metal batteries focus on preventing the formation of dendrites through control of the interface and Li nucleation[80], and several works have moved towards using extremely soft and flowable polymer coatings to stabilize the Li-metal anode[81-84] (discussed further below). Overall, it is becoming clear that mechanical properties are not the only factor to be taken into consideration when designing polymer electrolytes for Li-metal batteries.

In summary, the mechanical properties of poly-mers used in battery applications are key to achieving high-performance devices, but ideal mechanics must be combined with the appropriate polymer chemistry for optimal performance. For Si binders, elasticity combined with dynamic stress dissipation and self-healing has been shown to stabilize the cycling of large micrometre-sized Si particles. For Li-metal anodes, dendrite prevention can be pursued through the use of either a hard polymer electrolyte with a high modulus or softer materials with favourable Li-surface interactions. Full understanding of the requirements for polymer mechanics and the molec-ular characteristics that give rise to these properties is necessary for proper materials selection and design for high-performance devices.

Designing polymers for Li-ion transport

Solid polymer electrolytes (SPEs) have been the subject of intensive study for decades and have the potential to enable high-energy-density batteries based on advanced chemistries. Generally, solid-state batteries address the challenges of uncontrolled volume expansion, dendrite growth, unwanted side reactions, uncontrolled mass trans-port and thermal runaway[85]. Additionally, SPEs offer the advantage of being low cost, highly processable and easy to integrate into existing battery architectures when com-pared with ceramic solid electrolytes[86]. Existing reviews provide excellent descriptions of the mechanism of ion transport in SPEs and overviews of the numerous poly-mer compounds previously studied[87,88]. Here, we focus on polymer design principles for effective SPEs, including control of the crystallinity, glass transition temperature (T_g), dielectric constant and solvation site connectivity.

Overview of ion conduction in polymer electrolytes. PEO was first discovered to dissolve Li salts in 1973 (REFS[89,90]) and today is still one of the most intensely studied and widely used polymer electrolytes[91]. The mechanism for ion transport in polymer electrolytes involves the dissociation of a salt by the polymer back-bone and transport of the resulting ionic species via ion hopping or chain segmental motion (FIG. 4a). Generally, the ionic conductivity (σ) of an electrolyte is a product of the mobility (μ) at which the ions can move via the aforementioned mechanisms and the concentration of free charge carriers (c):

$$\sigma = \mu c \tag{1}$$

Given that ion transport through polymer electro-lytes is intimately coupled to the motion of the polymer backbone (FIG. 4a,b), it is not surprising that the depend-ence of ion conductivity on temperature can be described by the empirical Williams–Landel–Ferry relationship developed for describing the viscosity of polymer melts[92]. These equations governing polymer viscosity can be for-mulated into the more specific Vogel, Tamman and Fulcher relationship (equation 2), which is widely used to describe ion motion in polymer melts[93-95].

$$\sigma = A \exp\left[\frac{-E_a}{R(T-T_0)}\right] \tag{2}$$

Here, E_a is a pseudo-activation energy for ion motion, A is a pre-exponential factor, T is the tempera-ture, T_0 is a reference temperature and R is the gas con-stant. Although the reference temperature has an arbitrary value in the original Williams–Landel–Ferry equation, it is typically taken to be 50 K below the T_g when describing ion transport[96]. This temperature, $T_g - 50$ K, is experimentally observed to be the temper-ature at which the configurational entropy or free vol-ume of the polymer becomes effectively zero[97,98]. The Vogel–Tamman–Fulcher equation provides qualita-tively accurate descriptions of ion transport in many studies; however, the precise meanings of the constants are not clear, and recent studies have shown that the two descriptors (E_a and A) are coupled when describing ion transport[99].
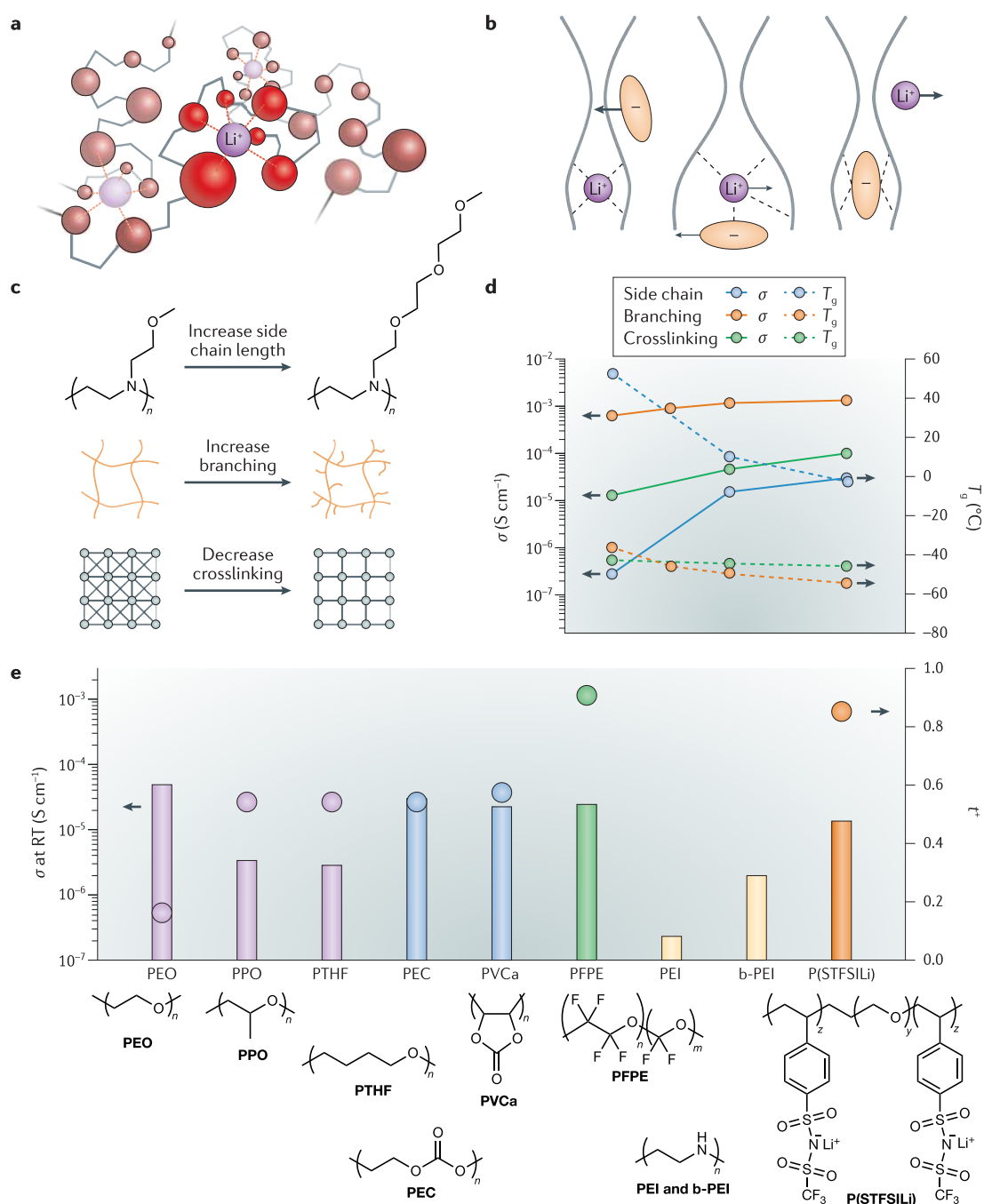
Fig. 4 | **Ion transport in polymer electrolytes. a** | Illustration of ion transport via Li⁺ hopping from one solvation site to another in poly(ethylene oxide) (PEO). The red dashed lines indicate Li⁺ (purple) solvation by O atoms (red) of the PEO polymer; the O atoms shown in bright red are actively solvating Li⁺. The transparent purple circles are potential solvation sites for Li⁺ to hop into. **b** | Schematic showing salt solvation by a polymer backbone. The arrows indicate the motion of the cation or anion with the thickness of the arrow indicating the relative mobility of each species. The three distinct cases are excessive Li⁺–polymer coordination (left), loose Li⁺–polymer coordination (centre) and selective anion solvation (right). The degree of solvation of the cation influences the transference number (t^+) and overall Li-ion conductivity. **c** | Polymer modifications that lower the glass transition temperature (T_g) and lead to higher ionic conductivity (σ) include increasing the length of the polymer side chain, increasing the amount of branching in a crosslinked polymer and decreasing the degree of crosslinking. **d** | Experimental data show the effects of polymer design on T_g (dashed lines) and σ (solid lines). **e** | A comparison of the room-temperature (RT) σ and t^+ of polymer electrolytes with different polymer backbones. The polymers are categorized according to the functional groups in the backbone: ethers (purple; poly(ethylene glycol) (PEG)[121,214], poly(propylene oxide) (PPO)[215,216] and poly(tetrahydrofuran) (PTHF)[114]), carbonates (blue; poly(ethylene carbonate) (PEC)[112] and poly(vinylene carbonate) (PVCa)[217]), fluorinated backbones (green; perfluoropolyether (PFPE)[117]), nitrogen heteroatoms (yellow; poly(ethylenimine) (PEI)[218] and branched-poly(ethylenimine) (b-PEI)[219]) and single-ion conductors (red; lithium poly(4-styrenesulfonyl(trifluoromethylsulfonyl)imide) (P(STFSILi)–block-PEO[71]). Panel **d** data from REFS[77,103,213].

In addition to the overall ionic conductivity, the transference number of polymer electrolytes is an important figure of merit when assessing their efficacy in Li-ion batteries. The transference number (t^+) in a binary electrolyte (equation 3) is the ratio of the cation mobility (μ^+) to the total ion migration within the electrolyte ($\mu^+ + \mu^-$, where μ^- is the anion mobility) in response to an electric field. Ideally, the transference number will be unity, as transport of the redox-inactive anion results in concentration polarization across the cell, which increases the charge overpotential and limits the rate capability of the battery[100].

$$t^+ = \frac{\mu^+}{\mu^+ + \mu^-} \qquad (3)$$

Designing polymers for effective Li-ion transport. When attempting to increase the conductivity of polymer electrolytes, lowering the T_g of the polymer backbone provides a tractable handle to improve performance (FIG. 4c,d). Additionally, it is widely accepted that ion conduction in polymers occurs in the amorphous regions except for in specific instances[101,102]. Consequently, a major design goal for polymer electrolytes is to increase the amorphous phase of the polymer by reducing crystallinity. In a salient example of the influence of T_g on ionic conductivity, a series of polymers was synthesized with identical backbone chemistry but with increasing side-chain lengths and thus different values of T_g (FIG. 4c). When the length of the side chain increased from one to three repeat units, the corresponding ionic conductivity increased tenfold[103]. Side-chain engineering provides only one method for tuning the T_g of an ion-conducting polymer[104]; other strategies to suppress crystallinity and reduce the T_g of polymer electrolytes include increasing polymer branching, decreasing the degree of crosslinking (FIG. 4c) and synthesizing hyperbranched polymers[105] or bottlebrush polymers[106].

Lowering the T_g of the electrolyte matrix increases the ionic conductivity of an SPE, but it does not affect the core transport mechanism of Li$^+$ through the PEO membrane. Ion conduction within an SPE is governed by the degree of salt dissociation and the coordination environment of Li$^+$ in the polymer backbone. Substantial work has been devoted to developing 'superionic' polymer conductors, in which the ion transport is decoupled from the segmental relaxation of the polymer chain[107,108]. These works demonstrate how the frustrated packing of rigid polymers causes an excess of free volume, enabling faster ion transport than would be expected based on the T_g of the polymer[109,110].

Increasing the dielectric constant of a polymer increases the degree of salt dissociation, whereas the coordination of Li$^+$ is typically stronger in polymers with Lewis basic functional groups (that is, with higher donor numbers)[111]. Although rigorous studies exploring the effect of polymer dielectric constant and donor number on ionic conductivity are lacking, it is known that ion solvation can either be too strong, in which case the ion is adhered to the polymer backbone and thus immobile, or too weak, in which case the salt does not dissociate. PEO with lithium bis(trifluoromethane)sulfonimide (LiTFSI)

has a transference number of 0.2, which indicates that the coordination environment of the PEO medium is too strong (FIG. 4e). In an effort to overcome this strong coordination, several loosely coordinating polymer electrolytes with higher transference numbers have been investigated[86] (FIG. 4e). These polymer backbones are based on poly(ethylene carbonate)[112,113], poly(tetrahydrofuran)[114], polyesters[115], perfluoropolyethers[116,117] and polyphosphazenes[118] (FIG. 4e). In a recent computational study, a series of polyborane SPEs that incorporate heteroatoms with Lewis acidity in the backbone were proposed[119]. The incorporation of heteroatoms enables the polyboranes to selectively solvate TFSI$^-$ rather than Li$^+$, leading to greatly enhanced Li$^+$ motion (FIG. 4b). Although the feasibility of synthesizing such compounds is yet to be established, such a strategy is promising for overcoming excessive Li$^+$ coordination in SPEs.

The concept of connectivity has been proposed as a way of describing the number of favourable Li$^+$ solvation sites available to which the cation can move from its current solvation site[120]. It was shown that discrepancies between ionic conductivity and T_g can be accounted for when the connectivity of solvation sites in the SPE is considered[121]. For efficient ion transport through a solid electrolyte, it is beneficial to have homogeneous solvation sites that are in close proximity to each other. It is for this reason that relatively chemically simple polymer electrolytes such as PEO are so effective.

Several single-ion-conducting SPEs have been developed to improve upon the low transference number in the conventional PEO electrolyte ($t^+ \approx 0.2$). Typically, these electrolytes use a Li salt in which the anion is covalently attached to the polymer backbone. The most notable example of a single-ion conductor is a block copolymer with a PEO ion-conducting block and a lithium poly(4-styrenesulfonyl(trifluoromethylsulfonyl)imide) (P(STFSILi)) block[71] (FIG. 4e). In this case, the tethered anion is immobile, leading to a transference number near unity. Other strategies for creating SPEs with high transference numbers are crosslinking a methacrylated Li salt into a PEO network[122] and mixing Li-containing nanoparticles into the polymer matrix[123]. Such efforts have produced polymer electrolytes with high transference numbers but with very low ionic conductivities in the absence of a liquid plasticizer. The low conductivity is attributed to a strong ion pairing between Li$^+$ and the polyanion backbone and the reduction in the contribution of the anion to the overall conductivity[124].

To design an effective SPE, it is important to design an amorphous polymer system with domains that have high segmental motion while also balancing the solvation of Li$^+$ and the connectivity of solvation sites. In a practical application, it will be imperative to also have a high transference number. Finally, these properties should be carefully considered with respect to the mechanical stability and electrochemical stability, which are the primary benefits of transitioning to solid-state devices.

Electrochemical stability considerations. In addition to ion transport properties, the electrochemical stability of the electrolyte needs to be considered to ensure that the electrolyte is compatible with both of the electrodes.

Typically, cyclic voltammetry experiments are used to determine the electrochemical stability window of a material. However, these sweeps are usually performed between two stainless-steel blocking electrodes. Using this method, the stability window is typically overestimated because the conductive carbon additives and active materials contained in real composite electrodes can promote decomposition reactions[125]. To improve this characterization, leakage current measurements can be performed using the actual cell configuration to obtain more precise data[126]. Generally, the electrochemical stability window of polymers can be extended by lowering the highest occupied molecular orbital (HOMO) and raising the lowest unoccupied molecular orbital (LUMO), but it is important to note that the energy levels of these orbitals do not equate to the redox potentials of the material[127], and this correlation should be used only as a rough guideline for material design. Ideally, new descriptors will be identified that directly relate polymer structure to the reduction and oxidation potentials.

Polymer design for electron transport

Molecular design of electronically conducting polymers. Conventional polymer materials are electronically insulating. However, when the π orbitals are conjugated along a large macromolecule, the electronic energy levels increase in density and approximate the band structure of an inorganic semiconductor[128,129] (FIG. 5a). The addition of dopants can inject either holes into the HOMO (p-type doping) or electrons into the LUMO (n-type doping) to create free charge carriers that move along the polymer backbone and hop between polymer chains, rendering metallic behaviour and high electronic conductivity[130]. Intensive research over the past 50 years has led to the development of many conducting and semiconducting polymers[129]. In batteries, electronically conducting polymers have been used to improve the kinetics of charge transport in composite electrodes.

Conductive polymers for the Si anode. Traditionally, Si anodes consist of Si active material, an insulating binder and conductive carbon black (FIG. 5b, left panel). These additives are disadvantageous because they lower the overall specific capacity of the electrode, and owing to the large volume expansion of Si, the electrical connection to the conductive carbon is readily lost. To minimize these drawbacks, conductive polymers have been proposed to serve as binders while simultaneously providing continuous electron transport pathways throughout the electrode[4] (FIG. 5b, right panel). There are many requirements to be considered when replacing the binder and conductive additive with a single conductive polymer, including the overall conductivity and bandgap of the polymer. However, the benefit of using polymers for this application is that they can be rationally tailored to meet the design parameters. One effective way to accomplish this is to modify a basic linear polymer with side chains that change the solubility, packing and energy levels[131] (FIG. 5c). Adding polar ether groups as side chains improves cycling owing to faster ion transport through the composite electrode[132,133] (FIG. 5d). However,

although the introduction of polar groups increases the uptake of the electrolyte, too many polar groups can cause excessive swelling, which interferes with electron conduction in the polymer[134].

Owing to the low operating voltages of the Si anode (0.01–1.00 V versus Li/Li$^+$), de-doping of polymers with LUMOs above these potentials (that is, the transfer of charge out of the polymer) occurs, and the conductivity of these materials decreases[135]. The ideal conductive polymer for Si electrodes should have a low-lying LUMO so that is remains n-doped (that is, the polymer accepts electrons during the charging process) at low voltages. Electron-withdrawing groups attached to the conjugated backbone can be used to achieve highly conjugated polymers with the desired low-energy LUMO[136] (FIG. 5d). On the basis of this knowledge, a polyfluorene-based material was introduced with a tailored electronic state that prevented de-doping (FIG. 5e). It is noteworthy that the exact effects of tailoring the electronic properties of a polymer depend on the electrochemical environment[137]. In another example, a side chain functionalized with a Si-interacting moiety was used to increase the cohesion of the composite electrode[138]. There are also commercially available polymers that can maintain their electronic conductivity during battery operation, such as poly(3,4-ethylenedioxythiophene) (PEDOT)[139] (FIG. 5e). Therefore, although the design of conductive polymers is challenging, the modular nature of polymer synthesis offers a promising way to realize effective designs. For future work, it will be beneficial to identify conductive polymer binders that can be paired with cost-effective micrometre-sized Si particles.

Conductive polymers for S cathodes. Similar to Si anodes, S cathodes face the challenges of volume expansion, particle isolation and notable capacity fade upon cycling[140]. Although the volume change of S during cycling is not as severe as it is for Si, S and Li$_2$S are more electronically insulating than Si and thus require larger amounts of conductive carbon to obtain reasonable electrode activity[141]. Many of the design concepts for conductive polymers used for Si and S electrodes are the same; however, it is important to remember that reactions at the S cathode take place at higher potentials (2–3 V versus Li/Li$^+$), and thus the energy levels of the ideal polymer will be different.

Many conductive polymers have been used to enable S electrodes, including polyaniline (PANi)[142], polypyrrole (PPy)[143] and PEDOT[144] (FIG. 5e). In an early study, it was observed that coating a C–S nanocomposite with PEDOT:polystyrene sulfonate led to an increase in cycle life and better rate capability of the electrode owing to lower charge-transfer resistance between particles in the presence of the conductive polymer[145]. The importance of both low charge-transfer resistance and high surface area was shown by use of a highly soluble isoindigo-based conducting polymer with a conjugation-breaking pyridine group for coating onto a high-surface-area substrate[146]. The high conductivity and solubility of the isoindigo polymer allowed for the polymer content in the electrode to be minimized while still enabling high areal capacity and stable
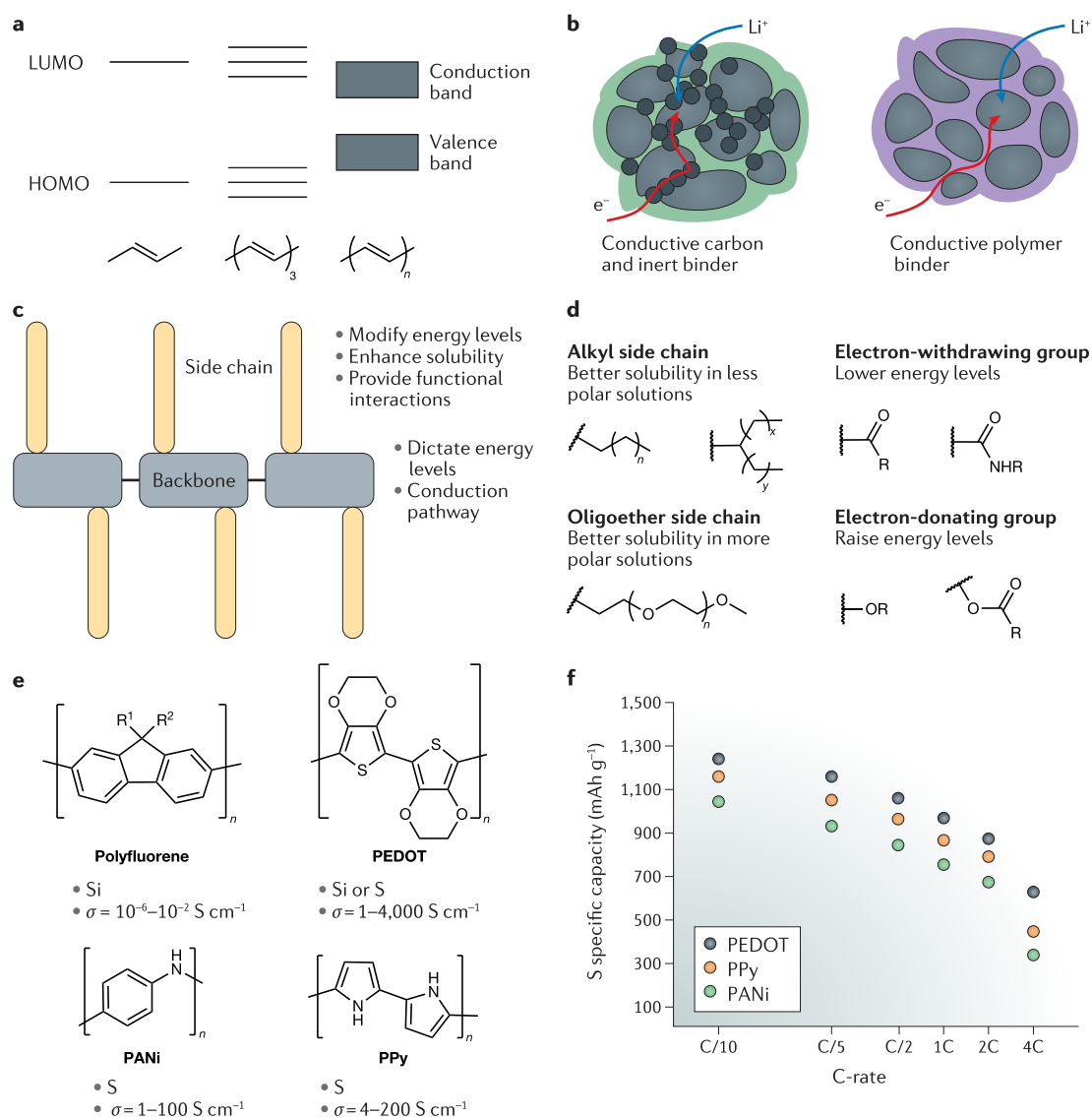
Fig. 5 | **Electronic conductivity in polymers. a** | The energy-level diagram displays how the energy levels are affected by conjugation. **b** | A comparison of charge transport through a traditional composite electrode with a polymer binder and conductive carbon (left) and through an electrode with a conductive polymer binder (right). **c** | Modifications to the polymer backbone and side chains can be used to control the properties of the material. **d** | Chemical structures of side chains used to modify conductive polymer backbones and their typical intended functions. **e** | Chemical structures of conductive polymers used as binders for Si and S electrodes and their electronic conductivity (σ). **f** | Plot of the specific capacity of S electrodes at various C-rates, showing that polymers with higher conductivities provide increased activation of the material and a better rate capability. HOMO, highest occupied molecular orbital; LUMO, lowest unoccupied molecular orbital; PANi, polyaniline; PEDOT, poly(3,4-ethylenedioxythiophene); PPy, polypyrrole. Panel **e** data from REFS[135,220–222]. Panel **f** data from REF.[144].

cycling of electrodes with a high S content of 90 wt%. Furthermore, it was demonstrated that the interconnectivity of PANi-based electrodes could be improved by swelling the polymer with *m*-cresol before mixing with the electrode-active materials. This swelling enables the polymer to disperse well with the C–S mixture, leading to lower charge-transfer resistance and superior battery performance than with non-conductive binders such as PVDF and poly(tetrafluoroethylene). Although conducting polymers are certainly useful for improving the performance of S cathodes, many of the studies cited above also included a PVDF binder in the final

electrode assembly. This is because, conventionally, the mechanical properties of conducting polymers are not sufficient to hold the S electrodes together. When used directly as a binder, it was found that PEDOT is a more effective binder than PVDF for S microparticles because of its greater affinity for the S species[147]. PEDOT was also found to enable increased activation of the S-active material as it has a higher conductivity than PANi and PPy, leading to increased specific capacity and improved rate capability (FIG. 5f).

Overall, there are many design considerations when using conducting polymers for Li-ion batteries.

Successful implementation of conducting polymers requires excellent compatibility between the energy levels of the polymer and the electrode material, fast electron transport properties and mechanical properties that are compatible with the electrode. Although the requirements for different active materials, in this case, Si and S, are different, the general design principles remain the same. The backbone of the conducting polymer mainly defines the energy levels and conductivity of the polymer, whereas the side chains help to tune the chemical interactions, molecular packing and energy levels for specific applications (FIG. 5c).

Designing interactions in polymers
In addition to the mechanical and transport properties of polymers used in battery applications, it is also necessary to consider the important chemical interactions and reactions that occur between the polymers and electrode species. Below, we focus on the design of polymers with specific functional reactive and/or interactive sites for trapping polysulfide species and stabilizing Si anodes.

Polymers for polysulfide trapping. As discussed above, the electronic conductivity of S and lithiated S species is poor, and various electronically conductive polymers have been used as binders to overcome this limitation. In addition to the issue of electronic conductivity, intermediate Li_2S_x ($2 < x < 8$) species can dissolve in commonly used organic electrolytes. To prevent this dissolution, which causes self-discharge, poor efficiency and low cycling stability, binders and conductive carbon additives have been designed to trap the polysulfide species through precise chemical interactions[4,42]. Specifically, in carbonaceous materials, it was found that heteroatom dopants, such as N, can strongly coordinate with Li in Li_2S_x (REFS[148,149]) and that S atoms can associate with S_x^{2-} (REF.[150]). Similar interactions were observed for polar functional groups containing N, O or S in polymer binders, leading to interaction strengths of ~1–2 eV with Li_2S_x, with stronger Li–X (X = N, O, S or other species) binding providing improved capacity retention[144,151–153] (FIG. 6a). Conjugated polymers have even been designed to take advantage of the ability of S to form organic compounds and to undergo in situ vulcanization to bind directly with excess S (REFS[154,155]).

Owing to the strong ionic character of polysulfide species, polyelectrolyte materials with a positive charge have been used as binders to trap S_x^{2-} (REFS[156,157]) (FIG. 6a), and negatively charged polymers have been coated onto the separator to repel the polysulfide species and prevent crossover[158,159]. As larger polysulfides are less ionic and do not bind to Li^+ as strongly as smaller polysulfides do, polyelectrolyte-based strategies are more effective at binding or repelling the larger polysulfide oligomers[156]. In the past few years, advanced polymer systems have been developed that combine multiple strategies to obtain electrodes with high mass loading and high S content. The incorporation of pyridine groups as either side chains or into the backbone of polymers increased the capacity retention compared with polymers without such groups. This modification also enabled high areal capacities and low binder content owing to the

enhanced processability of the conjugation-breaking pyridine groups, which increased the solubility of the polymer owing to increased backbone flexibility[146]. A benzoxazine-based polymer enabled in situ polymerization and vulcanization (FIG. 6a) to obtain high mass loading and long cycling stability[160].

When considering approaches for further improvements, it can be seen that S-binding groups share many similar characteristics with hydrogen-bond acceptors. Existing hydrogen-bond acceptors that have not yet been explored for polysulfide trapping could be low-hanging fruit for future study. The electron-donating nature of the polysulfide-trapping groups can hinder ion transport, but the development of specific binding sites may be a way to circumvent this issue[161]. Metal ions also coordinate strongly with polysulfide species, and this has been used to great effect in metal–organic frameworks and other metal-based structures[42]. Metal-ion-coordinated polymers could potentially be used as binders to trap polysulfides. Ideally, a polymer binder or separator coating designed to increase the cycling stability of the S cathode should strongly bind to the polysulfide species (using N, O, S or other electron-donating motifs), allow for electron transport (through a conjugated structure or low binder content) and enable Li-ion transport.

Chemical interactions in polymer binders for Si anodes. Good mechanical properties alone are not enough for a polymer binder to stabilize the Si electrode, and the chemical interactions between the binder and active material must also be considered. It was found that hydrogen bonding between the polymer binder and the oxide surface of the Si active material drastically improves the cycling stability[162] (FIG. 6b). Initially, CMC was used as the binder without a clear understanding of the origin of the improved cycling stability[60], but further study identified the interaction with the surface of the Si particles as the crucial factor enabling longer cycling lifetimes[163–165]. Subsequently, alginate[58] and PAA[59] were shown to have similar interactions with the Si surface and to provide improved cycling. The dynamic nature of the hydrogen bonding between the binder and active material is thought to provide a self-healing effect to the electrode, enabling the effective dissipation of stress and the maintenance of the composite structure. This understanding has led to a large body of work directed at modifying and enhancing the binder–Si interaction[52,53]. A series of modified carbohydrate polymers was synthesized for improved binder–Si adhesion using catechol[166], hyperbranched cyclodextrin[167] and branched bottlebrush structures[168]. Many of these hydrogen-bonding-based binders are processed in water, and it should be noted that the pH of the electrode slurry affects both the dispersion of the particles and the chemistry of the Si surface[163,169]. Thicker oxide layers on the Si particles result from slurries with a higher pH and likely lead to poorer cell performance[170]. This is evidenced by the generally worse performance of CMC (pH ~7) compared with PAA (pH ~3).

Tuning the interaction between polymers and the Si anode is also important for the design of non-traditional conductive polymer binders. For optimal
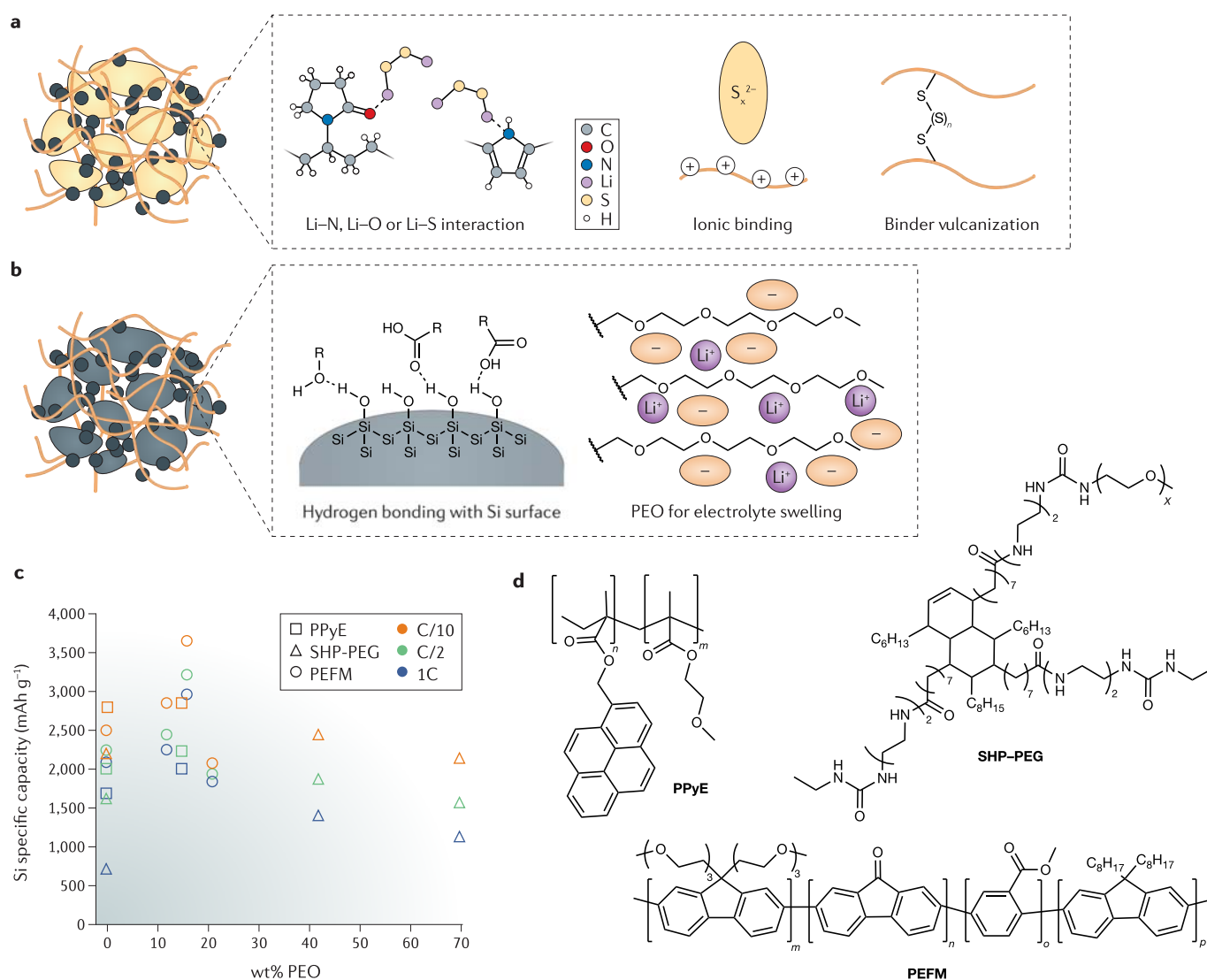
Fig. 6 | **Chemical interactions between S or Si and polymer binders. a** | The interaction between the polymer binder and S cathode can be designed to prevent the dissolution of polysulfide species from the cathode. Strategies include the formation of secondary interactions (that is, Li_2S_x–N, Li_2S_x–O and Li_2S_x–S ($2 < x < 8$)), ionic binding and covalent crosslinking. **b** | Desirable properties of a binder for Si anodes include strong adhesion to the Si particle surface through interactions such as hydrogen bonding and swelling with liquid electrolyte for fast Li^+ transport. **c** | Specific capacities of Si electrodes are shown at different C-rates for binders based on polypyridine ether (PPyE)[133], a self-healing polymer with poly(ethylene glycol) groups (SHP–PEG)[174] and a block copolymer with four different polymer blocks (PEFM)[134]. **d** | Chemical structures of the binders from panel **c**, illustrating how poly(ethylene oxide) (PEO) is introduced into the binders.

charge-transport properties, the Si particles will ideally be conformally coated with a conducting polymer. This has been successfully achieved with covalent anchoring of the binder by electropolymerizing PEDOT onto the surface of Si nanowires[171] and in situ polymerization of a crosslinked 3D PANi network around Si nanoparticles[172]. As discussed, ideal binders should also have both strong interactions with the Si surface and appropriate mechanical properties for stable cycling. Although these properties are difficult to achieve in conductive polymers alone, a dual-network structure has been shown in which a mechanically robust PAA matrix holds the Si nanoparticles together, and an in situ polymerized PANi network imparts high rate capability and enhanced cycle life[173].

In addition to strong interaction with the Si surface, the binder should have good interaction with the electrolyte to wet the composite electrode, which is necessary to enable fast ion transport and thereby fast charging kinetics. To this end, polar PEO-based side chains have been added to nonpolar self-healing[174] or conductive polymer[132,133] binders (FIG. 6b) to improve the interaction of the polymers with the electrolyte and enable higher currents (FIG. 6c,d). However, a peak performance enhancement is observed at ~15 wt% PEO added to the binder (FIG. 6c), which is likely due to a dilution of the other beneficial binder properties such as adhesion or electronic conductivity. Even polar, PAA-based binders have benefited from the addition of PEO groups for improved swelling and ion transport[24].

In combination with the conclusions from the above discussion of binder mechanics, it is possible to identify common features of effective reported binders, including hydrogen-bonding groups to reversibly bind with the surface of the Si particles, a dynamic networked structure for mechanical stability of the electrode and strong interactions with the electrolyte and Li^{+} for fast ion transport[53]. This combination has been demonstrated in two PAA-based binders[24,67] and a fatty acid self-healing polymer[23] and has enabled stable long-term cycling of large Si micrometre-sized particles at high mass loading.

When designing polymers with functional groups for specific interactions with species in the battery environment, it is important to identify the desired strength of interaction and the mechanism by which these interactions will take place. These parameters will then inform the chemical and structural design of the polymer material. For polysulfide binding, electron-donating N, O and S functional groups have proved most effective for trapping the soluble species and preventing crossover. In Si electrodes, strong adhesion to the active particles through hydrogen bonding with the oxide surface in an elastomeric binder has been demonstrated to be the most effective approach. Overall, a clear understanding of the relevant chemistry in the battery electrode is needed before design of the functionalized polymer materials can proceed.

Polymer design for stable interfaces

Owing to the harsh electrochemical environment of a battery, the electrolyte is generally thermodynamically unstable against one or both of the electrodes[175–177] (FIG. 7a). As a result of this instability, a layer of electrolyte decomposition products (known as the SEI) forms at the interface of the electrode and electrolyte. A large amount of work has gone into the study and understanding of the SEI, particularly in identifying its composition and structure[14,178–180]. Although each active material and electrolyte combination results in a different SEI, the general concept of improving the performance of the SEI to enhance cycling is common across all battery systems in which an SEI is present (at potentials <1 V and >4 V). The ideal SEI should be very thin, electronically insulating and ionically conductive. Additionally, the SEI should have high mechanical stability so that it does not crack during charging or discharging of the electrode.

Historically, the interface between the electrolyte and electrode has been studied almost exclusively on negative electrodes, beginning with graphite, moving to Si and, more recently, focusing on Li. However, the introduction of positive electrode materials that operate at higher voltages has prompted the study of electrolyte decomposition products on the cathode interface[176]. Carbonates are popular solvents for liquid electrolytes owing to their high dielectric constants, but standard carbonate mixtures do not form stable SEIs. Instead, fluoroethylene carbonate and vinylene carbonate are used as additives to help stabilize the SEI through the reductive formation of poly(vinyl carbonate)[181,182]. Ether-based electrolytes, however, result in SEIs that are polymeric in nature without the addition of additives[183].

Polymers at the electrode–electrolyte interface. In addition to providing cohesion to the composite electrode, polymer binders also affect the SEI that forms during cycling. For Si, binders that contain carboxylic acids are reduced to Li carboxylates, forming a protective layer on the active material that suppresses the reduction of the carbonate solvents[170]. In high-voltage $LiNi_{0.5}Mn_{1.5}O_4$-based electrodes, a polymeric silk protein was found to incorporate into the SEI, leading to decreased self-discharge and faster Li^{+} transfer through the SEI[184].

Although polymer electrolytes are promising alternatives to replace liquid electrolytes, the decomposition of polymer electrolytes is slower than that of liquids owing to slower reaction kinetics of the solid-state system. Nevertheless, an SEI still forms between the polymer and the electrode. Generally, carbonate-based and ether-based polymers decompose into Li alkyl carbonates and Li alkoxides, respectively, similar to those generated by liquid electrolytes[185,186]. The buried nature of the electrode–electrolyte interface has limited its study so far, especially with the use of powerful in situ techniques. Unfortunately, the oxidative stability of ether-based polymer electrolytes is limited to <4 V (REF.[87]), and new polymer electrolytes are needed that form a stable interface with high-voltage cathodes.

Polymer coatings on Li-metal electrodes. The polymeric nature of the SEIs that derive from liquid carbonate and ether electrolytes has prompted the development of polymer coatings (also called artificial SEIs) to stabilize the Li-metal electrode (FIG. 7b). A wide variety of polymers has been used for coatings, including ionomers[83,187,188], polydimethylsiloxane[82,189], PVDF[190], supramolecular polymers[81], elastomer composites[191] and poly(norbornene) with reactive ether functional groups[192] (FIG. 7c). These initial works yielded exciting results, but there were no clear design rules for synthesizing new coatings. A systematic study of varied polymer coatings led to the identification of key relationships between the polymer coatings and Li deposition[193]. Specifically, it was found that the exchange current of Li in the presence of a polymer coating can be predicted from the dielectric constant of the polymer coating. Moreover, through scaling analysis of the energetics of the nucleation process, it was found that the size of Li particles that grow during deposition increases with higher exchange currents and lower surface energies (FIG. 7b). Polymer coatings with a high dielectric constant or low surface energy also resulted in devices with higher Coulombic efficiencies (FIG. 7d).

These results can be used to identify two major classes of polymers that have been successfully used as artificial SEIs: siloxane-based polymers[82,189,193], which have a low surface energy and therefore promote the growth of large and dense Li deposits through interfacial interactions, and highly polar polymers and ionomers[83,187,188,190], which influence the ion transport through the coating and the overpotential of the deposition process. It has also been noted that an optimized thickness of these artificial SEIs is crucial to their favourable performance[188,193]. Taken together, these results suggest that the ideal polymer for an artificial SEI on a Li-metal electrode should have both
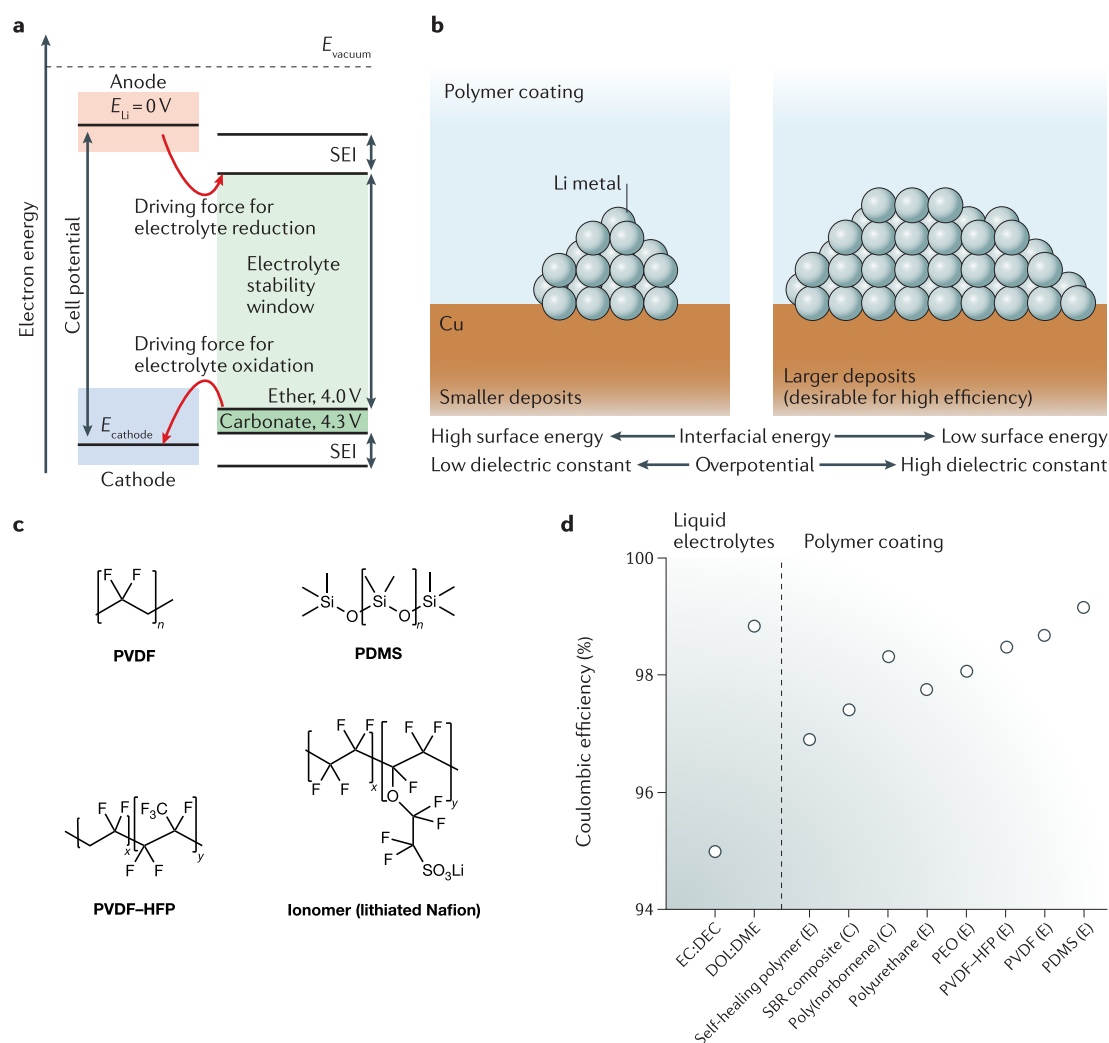
Fig. 7 | **Solid electrolyte and Li-metal interface in Li-ion batteries. a** | Energy-level diagram showing the electrochemical stability window of liquid electrolytes and the driving force for electrolyte decomposition (where $E_{cathode}$, E_{Li} and E_{vacuum} are the cathode, Li-anode and vacuum potentials, respectively). Decomposition products form a solid electrolyte interphase (SEI) that kinetically stabilizes the electrode–electrolyte interface. **b** | Desirable properties for polymer coatings used as artificial SEIs on Li-metal electrodes. **c** | Chemical structures of polymer coatings that have been shown to improve the quality of Li-metal deposition and the cycling efficiency of the cell. **d** | Coulombic efficiency of polymer coatings used as artificial SEIs and, for reference, common liquid electrolytes. Data are shown for a carbonate electrolyte (1 M LiPF$_6$ in ethylene carbonate (EC):diethyl carbonate (DEC) with 5 vol% fluoroethylene carbonate)[223], ether electrolyte (1 M lithium bis(trifluoromethanesulfonyl)imide in 1,3-dioxolane (DOL):1,2-dimethoxyethane (DME) with 1 wt% LiNO$_3$)[193], self-healing polymer[81], styrene butadiene rubber (SBR) composite[191], poly(norbornene)[192], poly(ethylene oxide) (PEO), poly(vinylidene fluoride–hexafluoropropylene) (PVDF–HFP), PVDF and polydimethylsiloxane (PDMS)[193]. Either an ether-based electrolyte (E) or a carbonate-based electrolyte (C) was used for electrochemical testing.

a high dielectric constant and low surface energy (FIG. 7b). Furthermore, the ability to deposit this ideal polymer coating from solution using a nonpolar, Li-compatible solvent is important for industrial production.

Designing polymers for safety
As the amount of energy stored in Li-ion batteries increases, so do the safety concerns associated with their operation. Unacceptable, catastrophic failure of batteries is common even with today's technology[31]. The consequences of battery failures are immense, from the perspectives of both user safety and economics. Thus, the development of improved safety mechanisms

for advanced battery chemistry is imperative. Polymers promise to have an important role in increasing the safety of batteries, primarily through their thermo-responsive properties or as non-flammable device components[31,194].

Thermoresponsive polymers are central to the safety mechanism in modern Li-ion batteries. The two most investigated temperature-responsive properties for creating safe batteries are polymer melting and thermal expansion[194]. These thermal properties can be controlled through modification of the monomer chemistry or polymer architecture. The melting temperature of a polymer can be increased by increasing the strength of
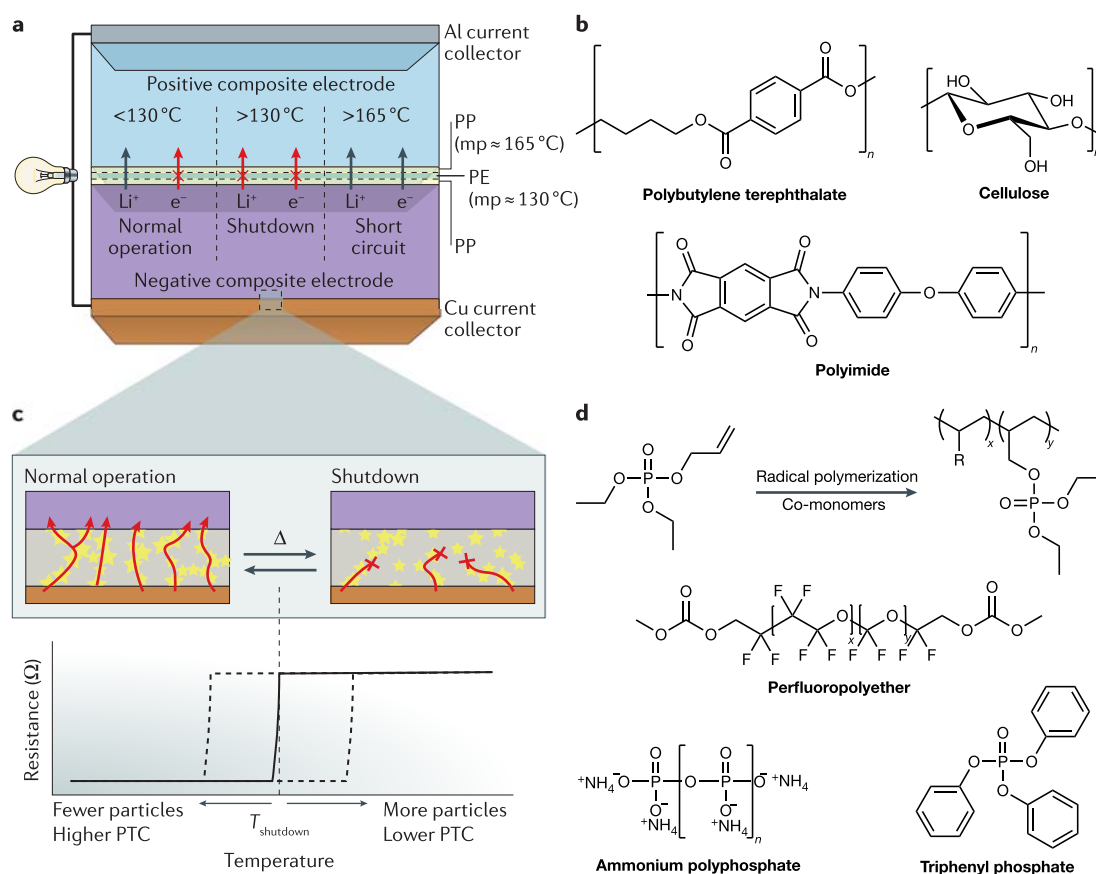
Fig. 8 | **Polymer materials for improved battery safety. a** | Diagram of a standard cell with a tri-layer polyolefin separator. Shutdown occurs if the polyethylene (PE) layer melts, but short circuit occurs upon melting of the polypropylene (PP) layers. **b** | Chemical structures of polymers used to fabricate separators with high thermal stability. **c** | Reversible operation of a thermoresponsive polymer composite (comprising PE and graphene-coated Ni microparticles) applied between the current collector and anode. The transition from normal operation to shutdown above the shutdown temperature ($T_{shutdown}$) owing to a large increase in resistance is shown. **d** | Chemical structures of flame-retardant polymers used as electrolytes and binders. mp, melting point; PTC, positive thermal expansion coefficient. Panel **c** is adapted from REF.[201], Springer Nature Limited.

interaction in the polymer backbone or by improving the ability of the polymer to pack into crystals (for example, by reducing chain flexibility, increasing symmetry or decreasing branching)[195]. The widely used Celgard separator contains a tri-layer structure of polypropylene–polyethylene–polypropylene. If the temperature of the battery exceeds the melting temperature of the polyethylene layer, ion transport through the battery is disabled, preventing thermal runaway[3] (FIG. 8a). One safety concern for this mechanism is that if the battery heats beyond 165 °C, the isotactic polypropylene layer will also melt, causing a short circuit in the battery. Although this shutdown feature does improve safety, polymer separators with high thermal stability have also been developed to help prevent the short circuiting that occurs upon melting of polypropylene[196–198] (FIG. 8b).

In addition to the melting separator, commercial cells are typically also equipped with an external resistor built with materials that have a positive thermal expansion coefficient (PTC), which stops current flow when heated to prevent thermal runaway. However, the speed at which thermal runaway occurs decreases the effectiveness of these external devices[194]. In polymers, the coefficient of thermal expansion correlates positively with the amorphous fraction of the polymer and inversely with T_g (REFS[199,200]). To improve upon external PTC resistors, a thermoresponsive polymer composite was developed based on polyethylene and graphene-coated nickel microparticles to be applied directly to the current collector of the cell[201] (FIG. 8c). Upon heating, the expansion of polyethylene causes the particles to move away from each other and to disconnect the percolated electron transport pathways. By tuning the content of nickel particles in the composite and the thermal expansion coefficient of the polymer matrix, the shutdown temperature can be tuned between 50 °C and 100 °C. Furthermore, upon cooling of the polymer matrix, battery operation resumes. This reversible safety switch is an attractive feature to implement in Li-ion batteries.

The thermal response of polymer solutions can also be used to increase the safety of Li-ion battery operation. Lower critical solution temperature (LCST) behaviour is observed in many polymer solutions owing to a negative entropy of mixing; thus, as the temperature increases, the interaction between the polymer and solvent becomes less favourable, and the solution begins to phase separate. The LCST behaviour in electrolytes consisting of poly(benzyl methacrylate) in an ionic liquid[202] and

methyl cellulose in aqueous solution[203] has been used to mitigate thermal runaway in Li-ion batteries. When heated, the polymer in these solutions separates from the solvent and forms an insulating phase or causes the electrolyte to gel, both of which reduce the ionic conductivity. Despite these efforts, taking advantage of the phase separation of thermoresponsive polymers does not result in complete cessation of battery operation. Therefore, at present, the thermal expansion or melting methods of preventing thermal runaway are preferred.

Developing materials that are intrinsically flame retardant is another central aspect of increasing Li-ion battery safety (FIG. 8d). Fireproof polymers are generally stiff and consist of fused rings or are highly halogenated[204]. Increasing the aromaticity of a polymer will also reduce its combustibility. Unfortunately, most of the polymer materials discussed in this Review are flammable, and, therefore, substantial work must be done on this front. Non-flammable oligomeric liquid electrolytes based on perfluoropolyether were demonstrated to enable good battery performance[117]. However, salt solubility is an issue in these highly fluorinated systems. In another example, a crosslinked gel polymer electrolyte was synthesized through radical polymerization with flame-retardant phosphate moieties linked into the polymer backbone[205]. In this electrolyte, the tethering of the flame-retardant moieties into the polymer backbone limits their effect on the electrochemical performance of the electrodes but results in gel electrolytes that are completely flame retardant even when swollen with a flammable liquid electrolyte. An electrospun core–shell microfibre separator consisting of a flame retardant (triphenyl phosphate) encapsulated by poly(vinylidene fluoride–hexafluoropropylene) releases the flame retardant when the melting temperature of the polymer is reached[206]. Recently, a binder based on a flame-retardant ammonium polyphosphate was used to reduce the overall flammability of the cell[207]. At present, it is difficult to incorporate flame-retardant moieties into electrolyte or binder materials without sacrificing performance, but there is no fundamental limitation preventing the development of flame-retardant polymers based on the principles described in earlier sections.

Conclusion and outlook
We have discussed the concepts and techniques used to design polymers for battery applications, describing how researchers are able to obtain polymers with specific mechanical, charge-transport and chemical properties and how these design principles apply to binders, electrolytes and functional coatings for Si, Li-metal and S advanced battery chemistries. These concepts were discussed separately, but in reality, advanced polymer materials used in high-performance devices require fine control of all these properties. Designing polymer electrolytes with high ionic conductivity requires careful consideration of crystallinity, T_g, polymer coordination and solvation site connectivity. For Si electrodes, carbohydrate polymers with a combination of elasticity and dynamic hydrogen bonding with the Si surface have been shown to be most successful at stabilizing inexpensive and high-efficiency micrometre-sized particles. Stabilizing Li-metal anodes requires design of the mechanics, surface chemistry and ion-transport properties, and the properties for an ideal material have yet to be fully understood. For S cathodes, electronically conductive polymers can increase the rate capability of the electrodes, and strongly binding polymers help to trap the soluble polysulfide species. For all these applications, safety is also a major concern.

Looking to the future, energy storage technologies will only continue to increase in importance as more renewable energy generation sources are deployed, electric vehicles capture a larger market share and portable electronics continue to become both smaller and more powerful. In order to continue to develop innovative solutions to present and future energy storage problems, research at the interface of polymer science and electrochemistry is crucial. As evidenced in this Review, work by researchers with experience in both fields and collaboration between experts in these respective areas have yielded important advances in enabling next-generation battery chemistries. Although new polymer materials will not single-handedly solve the challenges of next-generation energy technologies, they will certainly continue to have a key role moving forward.

Outstanding challenges for battery-related polymer materials include the development of fast room-temperature Li-ion transport, the further stabilization of high-capacity electrodes and improved electrochemical stability for high-voltage cathode materials. Promising approaches to resolve these and other issues could draw inspiration from recent trends in polymer science that include using highly specific sequence control to obtain well-defined structures[208], expanding control over materials properties through the use of secondary interactions[209,210] and designing new materials with recyclable chemistry[211] or bio-inspired architectures[212].

Published online: 03 April 2019

1. Chu, S., Cui, Y. & Liu, N. The path towards sustainable energy. Nat. Mater. 16, 16–22 (2017).
2. Nykvist, B. & Nilsson, M. Rapidly falling costs of battery packs for electric vehicles. Nat. Clim. Chang. 5, 329–332 (2015).
3. Arora, P. & Zhang, Z. J. Battery separators. Chem. Rev. 104, 4419–4462 (2004).
4. Chen, H. et al. Exploring chemical, mechanical, and electrical functionalities of binders for advanced energy-storage devices. Chem. Rev. 118, 8936–8982 (2018).
5. Obrovac, M. N. & Christensen, L. Structural changes in silicon anodes during lithium insertion/extraction. Electrochem. Solid State Lett. 7, A93–A96 (2004).
6. Obrovac, M. N. & Krause, L. J. Reversible cycling of crystalline silicon powder. J. Electrochem. Soc. 154, A103–A108 (2007).
7. Whittingham, M. S. History, evolution, and future status of energy storage. Proc. IEEE 100, 1518–1534 (2012).
8. Choi, J. W. & Aurbach, D. Promise and reality of post-lithium-ion batteries with high energy densities. Nat. Rev. Mater. 1, 16013 (2016).
9. Beaulieu, L. Y., Eberman, K. W., Turner, R. L., Krause, L. J. & Dahn, J. R. Colossal reversible volume changes in lithium alloys. Electrochem. Solid State Lett. 4, A137–A140 (2001).
10. Liu, X. H. et al. In situ atomic-scale imaging of electrochemical lithiation in silicon. Nat. Nanotechnol. 7, 749–756 (2012).
11. Lee, S. W., McDowell, M. T., Berla, L. A., Nix, W. D. & Cui, Y. Fracture of crystalline silicon nanopillars during electrochemical lithium insertion. Proc. Natl Acad. Sci. USA 109, 4080–4085 (2012).
12. Liu, X. H. et al. Size-dependent fracture of silicon nanoparticles during lithiation. ACS Nano 6, 1522–1531 (2012).
13. Saint, J. et al. Towards a fundamental understanding of the improved electrochemical performance of silicon–carbon composites. Adv. Funct. Mater. 17, 1765–1774 (2007).
14. Michan, A. L. et al. Solid electrolyte interphase growth and capacity loss in silicon electrodes. J. Am. Chem. Soc. 138, 7918–7931 (2016).

15. Ryu, J. H., Kim, J. W., Sung, Y.-E. & Oh, S. M. Failure modes of silicon powder negative electrode in lithium secondary batteries. *Electrochem. Solid State Lett.* **7**, A306–A309 (2004).

16. Chan, C. K. et al. High-performance lithium battery anodes using silicon nanowires. *Nat. Nanotechnol.* **3**, 31–35 (2008).

17. Liu, N. et al. A pomegranate-inspired nanoscale design for large-volume-change lithium battery anodes. *Nat. Nanotechnol.* **9**, 187–192 (2014).

18. Magasinski, A. et al. High-performance lithium-ion anodes using a hierarchical bottom-up approach. *Nat. Mater.* **9**, 353–358 (2010).

19. Beattie, S. D., Larcher, D., Morcrette, M., Simon, B. & Tarascon, J. M. Si electrodes for Li-ion batteries — a new way to look at an old problem. *J. Electrochem. Soc.* **155**, A158–A163 (2008).

20. Wu, M. et al. In situ formed Si nanoparticle network with micron-sized Si particles for lithium-ion battery anodes. *Nano Lett.* **13**, 5397–5402 (2013).

21. Li, Y. et al. Growth of conformal graphene cages on micrometre-sized silicon particles as stable battery anodes. *Nat. Energy* **1**, 15029 (2016).

22. Wang, C. et al. Self-healing chemistry enables the stable operation of silicon microparticle anodes for high-energy lithium-ion batteries. *Nat. Chem.* **5**, 1042–1048 (2013).

23. Chen, Z. et al. High-areal-capacity silicon electrodes with low-cost silicon particles based on spatial control of self-healing binder. *Adv. Energy Mater.* **5**, 1401826 (2015).

24. Choi, S., Kwon, T.-W., Coskun, A. & Choi, J. W. Highly elastic binders integrating polyrotaxanes for silicon microparticle anodes in lithium ion batteries. *Science* **357**, 279–283 (2017).

25. Xu, W. et al. Lithium metal anodes for rechargeable batteries. *Energy Environ. Sci.* **7**, 513–537 (2014).

26. Aurbach, D. & Cohen, Y. Morphological studies of Li deposition processes in LiAsF6/PC solutions by in situ atomic force microscopy. *J. Electrochem. Soc.* **144**, 3355–3360 (1997).

27. Aurbach, D., Zinigrad, E., Cohen, Y. & Teller, H. A short review of failure mechanisms of lithium metal and lithiated graphite anodes in liquid electrolyte solutions. *Solid State Ion.* **148**, 405–416 (2002).

28. Li, Z., Huang, J., Yann Liaw, B., Metzler, V. & Zhang, J. A review of lithium deposition in lithium-ion and lithium metal secondary batteries. *J. Power Sources* **254**, 168–182 (2014).

29. Lu, D. et al. Failure mechanism for fast-charged lithium metal batteries with liquid electrolytes. *Adv. Energy Mater.* **5**, 1400993 (2015).

30. Finegan, D. P. et al. In-operando high-speed tomography of lithium-ion batteries during thermal runaway. *Nat. Commun.* **6**, 6924 (2015).

31. Liu, K., Liu, Y., Lin, D., Pei, A. & Cui, Y. Materials for lithium-ion battery safety. *Sci. Adv.* **4**, eaas9820 (2018).

32. Crowther, O. & West, A. C. Effect of electrolyte composition on lithium dendrite growth. *J. Electrochem. Soc.* **155**, A806–A811 (2008).

33. Suo, L., Hu, Y.-S., Li, H., Armand, M. & Chen, L. A new class of solvent-in-salt electrolyte for high-energy rechargeable metallic lithium batteries. *Nat. Commun.* **4**, 1481 (2013).

34. Qian, J. et al. High rate and stable cycling of lithium metal anode. *Nat. Commun.* **6**, 6362 (2015).

35. Chen, S. et al. High-efficiency lithium metal batteries with fire-retardant electrolytes. *Joule* **2**, 1548–1558 (2018).

36. Suo, L. et al. Fluorine-donating electrolytes enable highly reversible 5-V-class Li metal batteries. *Proc. Natl Acad. Sci. USA* **115**, 1156–1161 (2018).

37. Fan, X. et al. Highly fluorinated interphases enable high-voltage Li-metal batteries. *Chem* **4**, 174–185 (2018).

38. Lu, Y., Tu, Z. & Archer, L. A. Stable lithium electrodeposition in liquid and nanoporous solid electrolytes. *Nat. Mater.* **13**, 961–969 (2014).

39. Ding, F. et al. Dendrite-free lithium deposition via self-healing electrostatic shield mechanism. *J. Am. Chem. Soc.* **135**, 4450–4456 (2013).

40. Shi, F. et al. Strong texturing of lithium metal in batteries. *Proc. Natl Acad. Sci. USA* **114**, 12138–12143 (2017).

41. Bruce, P. G., Freunberger, S. A., Hardwick, L. J. & Tarascon, J.-M. Li–O2 and Li–S batteries with high energy storage. *Nat. Mater.* **11**, 19–29 (2012).

42. Pang, Q., Liang, X., Kwok, C. Y. & Nazar, L. F. Advances in lithium–sulfur batteries based on multifunctional cathodes and electrolytes. *Nat. Energy* **1**, 16132 (2016).

43. Zhang, X. et al. Advances in lithium–sulfur batteries. *Mater. Sci. Eng. R. Rep.* **121**, 1–29 (2017).

44. Sun, Y., Liu, N. & Cui, Y. Promises and challenges of nanomaterials for lithium-based rechargeable batteries. *Nat. Energy* **1**, 16071 (2016).

45. Sperling, L. H. *Introduction to Physical Polymer Science* 557–612 (John Wiley & Sons, 2005).

46. Callister, W. D. Jr & Rethwisch, D. G. *Fundamentals of Materials Science and Engineering: an Integrated Approach* 147–196 (John Wiley & Sons, 2012).

47. Zhang, L., Zhang, L., Chai, L., Xue, P. & Hao, W. A coordinately cross-linked polymeric network as a functional binder for high-performance silicon submicro-particle anodes in lithium ion batteries. *J. Mater. Chem. A* **2**, 19036–19045 (2014).

48. Yoon, J., Oh, D. X., Jo, C., Lee, J. & Hwang, D. S. Improvement of desolvation and resilience of alginate binders for Si-based anodes in a lithium ion battery by calcium-mediated cross-linking. *Phys. Chem. Chem. Phys.* **16**, 25628–25635 (2014).

49. Ying, H., Zhang, Y. & Cheng, J. Dynamic urea bond for the design of reversible and self-healing polymers. *Nat. Commun.* **5**, 3218 (2014).

50. Chen, Z., Christensen, L. & Dahn, J. R. Large-volume-change electrodes for Li-ion batteries of amorphous alloy particles held by elastomeric tethers. *Electrochem. Commun.* **5**, 919–923 (2003).

51. Mazouzi, D. et al. Critical roles of binders and formulation at multiscales of silicon-based composite electrodes. *J. Power Sources* **280**, 533–549 (2015).

52. Shi, Y., Zhou, X. & Yu, G. Material and structural design of novel binder systems for high-energy, high-power lithium-ion batteries. *Acc. Chem. Res.* **50**, 2642–2652 (2017).

53. Kwon, T.-W., Choi, J. W. & Coskun, A. The emerging era of supramolecular polymeric binders in silicon anodes. *Chem. Soc. Rev.* **47**, 2145–2164 (2018).

54. Kim, J. S. et al. Effect of polyimide binder on electrochemical characteristics of surface-modified silicon anode for lithium ion batteries. *J. Power Sources* **244**, 521–526 (2013).

55. Sperling, L. H. *Introduction to Physical Polymer Science* 427–505 (John Wiley & Sons, 2005).

56. Chen, Z., Christensen, L. & Dahn, J. R. Comparison of PVDF and PVDF-TFE-P as binders for electrode materials showing large volume changes in lithium-ion batteries. *J. Electrochem. Soc.* **150**, A1073–A1078 (2003).

57. Liu, W.-R., Yang, M.-H., Wu, H.-C., Chiao, S. M. & Wu, N.-L. Enhanced cycle life of Si anode for Li-ion batteries by using modified elastomeric binder. *Electrochem. Solid State Lett.* **8**, A100–A103 (2005).

58. Kovalenko, I. et al. A major constituent of brown algae for use in high-capacity Li-ion batteries. *Science* **334**, 75–79 (2011).

59. Magasinski, A. et al. Toward efficient binders for Li-ion battery Si-based anodes: polyacrylic acid. *ACS Appl. Mater. Interfaces* **2**, 3004–3010 (2010).

60. Li, J., Lewis, R. B. & Dahn, J. R. Sodium carboxymethyl cellulose a potential binder for Si negative electrodes for Li-ion batteries. *Electrochem. Solid State Lett.* **10**, A17–A20 (2007).

61. Koo, B. et al. A highly cross-linked polymeric binder for high-performance silicon negative electrodes in lithium ion batteries. *Angew. Chem. Int. Ed.* **51**, 8762–8767 (2012).

62. Song, J. et al. Interpenetrated gel polymer binder for high-performance silicon anodes in lithium-ion batteries. *Adv. Funct. Mater.* **24**, 5904–5910 (2014).

63. Wei, L. & Hou, Z. High performance polymer binders inspired by chemical functions of textiles for silicon anodes in lithium ion batteries. *J. Mater. Chem. A* **5**, 22156–22162 (2017).

64. Zhu, X. et al. A highly stretchable cross-linked polyacrylamide hydrogel as an effective binder for silicon and sulfur electrodes toward durable lithium-ion storage. *Adv. Funct. Mater.* **28**, 1705015 (2018).

65. Kwon, T.-W. et al. Dynamic cross-linking of polymeric binders based on host-guest interactions for silicon anodes in lithium ion batteries. *ACS Nano* **9**, 11317–11324 (2015).

66. Kwon, T.-W. et al. Systematic molecular-level design of binders incorporating Meldrum's acid for silicon anodes in lithium rechargeable batteries. *Adv. Mater.* **26**, 7979–7985 (2014).

67. Xu, Z. et al. Silicon microparticle anodes with self-healing multiple network binder. *Joule* **2**, 950–961 (2018).

68. Lopez, J. et al. The effects of cross-linking in a supramolecular binder on cycle life in silicon microparticle anodes. *ACS Appl. Mater. Interfaces* **8**, 2318–2324 (2016).

69. Monroe, C. & Newman, J. The impact of elastic deformation on deposition kinetics at lithium/polymer interfaces. *J. Electrochem. Soc.* **152**, A396–A404 (2005).

70. Stone, G. M. et al. Resolution of the modulus versus adhesion dilemma in solid polymer electrolytes for rechargeable lithium metal batteries. *J. Electrochem. Soc.* **159**, A222–A227 (2012).

71. Bouchet, R. et al. Single-ion BAB triblock copolymers as highly efficient electrolytes for lithium-metal batteries. *Nat. Mater.* **12**, 452–457 (2013).

72. Gurevitch, I. et al. Nanocomposites of titanium dioxide and polystyrene-poly(ethylene oxide) block copolymer as solid-state electrolytes for lithium metal batteries. *J. Electrochem. Soc.* **160**, A1611–A1617 (2013).

73. Tung, S.-O., Ho, S., Yang, M., Zhang, R. & Kotov, N. A. A dendrite-suppressing composite ion conductor from aramid nanofibres. *Nat. Commun.* **6**, 6152 (2015).

74. Choudhury, S., Mangal, R., Agrawal, A. & Archer, L. A. A highly reversible room-temperature lithium metal battery based on crosslinked hairy nanoparticles. *Nat. Commun.* **6**, 10101 (2015).

75. Khurana, R., Schaefer, J. L., Archer, L. A. & Coates, G. W. Suppression of lithium dendrite growth using cross-linked polyethylene/poly(ethylene oxide) electrolytes: a new approach for practical lithium-metal polymer batteries. *J. Am. Chem. Soc.* **136**, 7395–7402 (2014).

76. Lu, Q. et al. Dendrite-free, high-rate, long-life lithium metal batteries with a 3D cross-linked network polymer electrolyte. *Adv. Mater.* **29**, 1604460 (2017).

77. Pan, Q., Smith, D. M., Qi, H., Wang, S. & Li, C. Y. Hybrid electrolytes with controlled network structures for lithium metal batteries. *Adv. Mater.* **27**, 5995–6001 (2015).

78. Tikekar, M. D., Archer, L. A. & Koch, D. L. Stabilizing electrodeposition in elastic solid electrolytes containing immobilized anions. *Sci. Adv.* **2**, e1600320 (2016).

79. Choudhury, S. et al. Confining electrodeposition of metals in structured electrolytes. *Proc. Natl Acad. Sci. USA* **115**, 6620–6625 (2018).

80. Lin, D., Liu, Y. & Cui, Y. Reviving the lithium metal anode for high-energy batteries. *Nat. Nanotechnol.* **12**, 194–206 (2017).

81. Zheng, G. et al. High-performance lithium metal negative electrode with a soft and flowable polymer coating. *ACS Energy Lett.* **1**, 1247–1255 (2016).

82. Liu, K. et al. Lithium metal anodes with an adaptive 'solid-liquid' interfacial protective layer. *J. Am. Chem. Soc.* **139**, 4815–4820 (2017).

83. Li, N.-W. et al. A flexible solid electrolyte interphase layer for long-life lithium metal anodes. *Angew. Chem. Int. Ed.* **57**, 1505–1509 (2018).

84. Liu, Y. et al. Transforming from planar to three-dimensional lithium with flowable interphase for solid lithium metal batteries. *Sci. Adv.* **3**, eaao0713 (2017).

85. Manthiram, A., Yu, X. & Wang, S. Lithium battery chemistries enabled by solid-state electrolytes. *Nat. Rev. Mater.* **2**, 16103 (2017).

86. Mindemark, J., Lacey, M. J., Bowden, T. & Brandell, D. Beyond PEO—alternative host materials for Li⁺-conducting solid polymer electrolytes. *Prog. Polym. Sci.* **81**, 114–143 (2018).

87. Hallinan, D. T. Jr & Balsara, N. P. Polymer electrolytes. *Annu. Rev. Mater. Res.* **43**, 503–525 (2013).

88. Long, L., Wang, S., Xiao, M. & Meng, Y. Polymer electrolytes for lithium polymer batteries. *J. Mater. Chem. A* **4**, 10038–10069 (2016).

89. Wright, P. V. Electrical conductivity in ionic complexes of poly (ethylene oxide). *Polym. Int.* **7**, 319–327 (1975).

90. Vashishta, P., Mundy, J. N. & Shenoy, G. K. (eds) *Fast Ion Transport in Solids* 87–107 (North-Holland, 1979).

91. Xue, Z., He, D. & Xie, X. Poly (ethylene oxide)-based electrolytes for lithium-ion batteries. *J. Mater. Chem. A* **3**, 19218–19253 (2015).

92. Williams, M. L., Landel, R. F. & Ferry, J. D. The temperature dependence of relaxation mechanisms in amorphous polymers and other glass-forming liquids. *J. Am. Chem. Soc.* **77**, 3701–3707 (1955).

93. Vogel, H. The temperature dependence law of the viscosity of fluids. *Phys. Z.* **22**, 645–646 (1921).

94. Fulcher, G. S. Analysis of recent measurements of the viscosity of glasses. *J. Am. Ceram. Soc.* **8**, 339–355 (1925).

95. Tammann, G. & Hesse, W. The dependancy of viscosity on temperature in hypothermic liquids. *Z. Anorg. Allg. Chem.* **156**, 245–257 (1926).

96. Ratner, M. A. & Shriver, D. F. Ion transport in solvent-free polymers. *Chem. Rev.* **88**, 109–124 (1988).

97. Adam, G. & Gibbs, J. H. On the temperature dependence of cooperative relaxation properties in glass-forming liquids. *J. Chem. Phys.* **43**, 139–146 (1965).

98. Cohen, M. H. & Turnbull, D. Molecular transport in liquids and glasses. *J. Chem. Phys.* **31**, 1164–1169 (1959).

99. Diederichsen, K. M., Buss, H. G. & McCloskey, B. D. The compensation effect in the Vogel–Tammann–Fulcher (VTF) equation for polymer-based electrolytes. *Macromolecules* **50**, 3831–3840 (2017).

100. Diederichsen, K. M., McShane, E. J. & McCloskey, B. D. Promising routes to a high Li⁺ transference number electrolyte for lithium ion batteries. *ACS Energy Lett.* **2**, 2563–2575 (2017).

101. Gadjourova, Z., Andreev, Y. G., Tunstall, D. P. & Bruce, P. G. Ionic conductivity in crystalline polymer electrolytes. *Nature* **412**, 520–523 (2001).

102. Christie, A. M., Lilley, S. J., Staunton, E., Andreev, Y. G. & Bruce, P. G. Increasing the conductivity of crystalline polymer electrolytes. *Nature* **433**, 50–53 (2005).

103. Sun, J., Stone, G. M., Balsara, N. P. & Zuckermann, R. N. Structure–conductivity relationship for peptoid-based PEO–mimetic polymer electrolytes. *Macromolecules* **45**, 5151–5156 (2012).

104. Nishimoto, A., Agehara, K., Furuya, N., Watanabe, T. & Watanabe, M. High ionic conductivity of polyether-based network polymer electrolytes with hyperbranched side chains. *Macromolecules* **32**, 1541–1548 (1999).

105. Hawker, C. J., Chu, F., Pomery, P. J. & Hill, D. J. T. Hyperbranched poly(ethylene glycol)s: a new class of ion-conducting materials. *Macromolecules* **29**, 3831–3838 (1996).

106. Bates, C. M., Chang, A. B., Momčilović, N., Jones, S. C. & Grubbs, R. H. ABA triblock brush polymers: synthesis, self-assembly, conductivity, and rheological properties. *Macromolecules* **48**, 4967–4973 (2015).

107. Wang, Y. et al. Solid state ionics. *Solid State Ion.* **262**, 782–784 (2014).

108. Wei, X. & Shriver, D. F. Highly conductive polymer electrolytes containing rigid polymers. *Chem. Mater.* **10**, 2307–2308 (1998).

109. Wang, Y. et al. Decoupling of ionic transport from segmental relaxation in polymer electrolytes. *Phys. Rev. Lett.* **108**, 088303 (2012).

110. Wang, Y. et al. Examination of the fundamental relation between ionic transport and segmental relaxation in polymer electrolytes. *Polymer* **55**, 4067–4076 (2014).

111. Kim, C. S. & Oh, S. M. Importance of donor number in determining solvating ability of polymers and transport properties in gel-type polymer electrolytes. *Electrochim. Acta* **45**, 2101–2109 (2000).

112. Tominaga, Y. & Yamazaki, K. Fast Li-ion conduction in poly(ethylene carbonate)-based electrolytes and composites filled with TiO₂ nanoparticles. *Chem. Commun.* **50**, 4448–4450 (2014).

113. Kimura, K., Motomatsu, J. & Tominaga, Y. Correlation between solvation structure and ion-conductive behavior of concentrated poly(ethylene carbonate)-based electrolytes. *J. Phys. Chem. C* **120**, 12385–12391 (2016).

114. Mackanic, D. G. et al. Crosslinked poly(tetrahydrofuran) as a loosely coordinating polymer electrolyte. *Adv. Energy Mater.* **6**, 1800703 (2018).

115. Pesko, D. M. et al. Effect of monomer structure on ionic conductivity in a systematic set of polyester electrolytes. *Solid State Ion.* **289**, 118–124 (2016).

116. Devaux, D. et al. Crosslinked perfluoropolyether solid electrolytes for lithium ion transport. *Solid State Ion.* **310**, 71–80 (2017).

117. Wong, D. H. C. et al. Nonflammable perfluoropolyether-based electrolytes for lithium batteries. *Proc. Natl Acad. Sci. USA* **111**, 3327–3331 (2014).

118. Blonsky, P. M., Shriver, D. F., Austin, P. & Allcock, H. R. Polyphosphazene solid electrolytes. *J. Am. Chem. Soc.* **106**, 6854–6855 (1984).

119. Savoie, B. M., Webb, M. A. & Miller, T. F. III. Enhancing cation diffusion and suppressing anion diffusion via Lewis-acidic polymer electrolytes. *J. Phys. Chem. Lett.* **8**, 641–646 (2017).

120. Webb, M. A. et al. Systematic computational and experimental investigation of lithium-ion transport mechanisms in polyester-based polymer electrolytes. *ACS Cent. Sci.* **1**, 198–205 (2015).

121. Pesko, D. M. et al. Universal relationship between conductivity and solvation-site connectivity in ether-based polymer electrolytes. *Macromolecules* **49**, 5244–5255 (2016).

122. Porcarelli, L. et al. Single-ion conducting polymer electrolytes for lithium metal polymer batteries that operate at ambient temperature. *ACS Energy Lett.* **1**, 678–682 (2016).

123. Villaluenga, I. et al. Nanostructured single-ion-conducting hybrid electrolytes based on salty nanoparticles and block copolymers. *Macromolecules* **50**, 1998–2005 (2017).

124. Ryu, S.-W. et al. Effect of counter ion placement on conductivity in single-ion conducting block copolymer electrolytes. *J. Electrochem. Soc.* **152**, A158–A163 (2005).

125. Xia, Y., Fujieda, T., Tatsumi, K., Prosini, P. P. & Sakai, T. Thermal and electrochemical stability of cathode materials in solid polymer electrolyte. *J. Power Sources* **92**, 234–243 (2001).

126. Zeng, X. et al. Kinetic study of parasitic reactions in lithium-ion batteries: a case study on LiNi₀.₆Mn₀.₂Co₀.₂O₂. *ACS Appl. Mater. Interfaces* **8**, 3446–3451 (2016).

127. Peljo, P. & Girault, H. H. Electrochemical potential window of battery electrolytes: the HOMO–LUMO misconception. *Energy Environ. Sci.* **11**, 2306–2309 (2018).

128. Hoffmann, R., Janiak, C. & Kollmar, C. A chemical approach to the orbitals of organic polymers. *Macromolecules* **24**, 3725–3746 (1991).

129. Heeger, A. J. Semiconducting polymers: the third generation. *Chem. Soc. Rev.* **39**, 2354–2371 (2010).

130. Heeger, A. J., Kivelson, S., Schrieffer, J. R. & Su, W. P. Solitons in conducting polymers. *Rev. Mod. Phys.* **60**, 781–850 (1988).

131. Mei, J. & Bao, Z. Side chain engineering in solution-processable conjugated polymers. *Chem. Mater.* **26**, 604–615 (2013).

132. Wu, H. et al. Toward an ideal polymer binder design for high-capacity battery anodes. *J. Am. Chem. Soc.* **135**, 12048–12056 (2013).

133. Park, S.-J. et al. Side-chain conducting and phase-separated polymeric binders for high-performance silicon anodes in lithium-ion batteries. *J. Am. Chem. Soc.* **137**, 2565–2571 (2015).

134. Wu, M. et al. Manipulating the polarity of conductive polymer binders for Si-based anodes in lithium-ion batteries. *J. Mater. Chem. A* **3**, 3651–3658 (2015).

135. Liu, G. et al. Polymers with tailored electronic structure for high capacity lithium battery electrodes. *Adv. Mater.* **23**, 4679–4683 (2011).

136. Kim, S. M., Kim, M. H., Choi, S. Y., Lee, J. G. & Jang, J. Poly(phenanthrenequinone) as a conductive binder for nano-sized silicon negative electrodes. *Energy Environ. Sci.* **8**, 1538–1543 (2015).

137. Song, C. K., Eckstein, B. J., Tam, T. L. D., Trahey, L. & Marks, T. J. Conjugated polymer energy level shifts in lithium-ion battery electrolytes. *ACS Appl. Mater. Interfaces* **6**, 19347–19354 (2014).

138. Zhao, H. et al. Mussel-inspired conductive polymer binder for Si-alloy anode in lithium-ion batteries. *ACS Appl. Mater. Interfaces* **10**, 5440–5446 (2018).

139. Higgins, T. M. et al. A commercial conducting polymer as both binder and conductive additive for silicon nanoparticle-based lithium-ion battery negative electrodes. *ACS Nano* **10**, 3702–3713 (2016).

140. Manthiram, A., Fu, Y. & Su, Y.-S. Challenges and prospects of lithium–sulfur batteries. *Acc. Chem. Res.* **46**, 1125–1134 (2012).

141. Seh, Z. W., Sun, Y., Zhang, Q. & Cui, Y. Designing high-energy lithium–sulfur batteries. *Chem. Soc. Rev.* **45**, 5605–5634 (2016).

142. Zhou, W., Yu, Y., Chen, H., DiSalvo, F. J. & Abruña, H. D. Yolk–shell structure of polyaniline-coated sulfur for lithium–sulfur batteries. *J. Am. Chem. Soc.* **135**, 16736–16743 (2013).

143. Liang, X. et al. Split-half-tubular polypyrrole@sulfur@polypyrrole composite with a novel three-layer-3D structure as cathode for lithium/sulfur batteries. *Nano Energy* **11**, 587–599 (2015).

144. Li, W. et al. Understanding the role of different conductive polymers in improving the nanostructured sulfur cathode performance. *Nano Lett.* **13**, 5534–5540 (2013).

145. Yang, Y. et al. Improving the performance of lithium–sulfur batteries by conductive polymer coating. *ACS Nano* **5**, 9187–9193 (2011).

146. Tsao, Y. et al. Enhanced cycling stability of sulfur electrodes through effective binding of pyridine-functionalized polymer. *ACS Energy Lett.* **2**, 2454–2462 (2017).

147. Wang, Z., Chen, Y., Battaglia, V. & Liu, G. Improving the performance of lithium–sulfur batteries using conductive polymer and micrometric sulfur powder. *J. Mater. Res.* **29**, 1027–1033 (2014).

148. Song, J. et al. Nitrogen-doped mesoporous carbon promoted chemical adsorption of sulfur and fabrication of high-areal-capacity sulfur cathode with exceptional cycling stability for lithium-sulfur batteries. *Adv. Funct. Mater.* **24**, 1243–1250 (2013).

149. Song, J. et al. Strong lithium polysulfide chemisorption on electroactive sites of nitrogen-doped carbon composites for high-performance lithium-sulfur battery cathodes. *Angew. Chem. Int. Ed.* **127**, 4399–4403 (2015).

150. Pang, Q. et al. A nitrogen and sulfur dual-doped carbon derived from polyrhodanine@cellulose for advanced lithium-sulfur batteries. *Adv. Mater.* **27**, 6021–6028 (2015).

151. Seh, Z. W. et al. Stable cycling of lithium sulfide cathodes through strong affinity with a bifunctional binder. *Chem. Sci.* **4**, 3673–3677 (2013).

152. Ma, L. et al. Tethered molecular sorbents: enabling metal-sulfur battery cathodes. *Adv. Energy Mater.* **4**, 1400390 (2014).

153. Park, K. et al. Trapping lithium polysulfides of a Li–S battery by forming lithium bonds in a polymer matrix. *Energy Environ. Sci.* **8**, 2389–2395 (2015).

154. Xiao, L. et al. A soft approach to encapsulate sulfur: polyaniline nanotubes for lithium-sulfur batteries with long cycle life. *Adv. Mater.* **24**, 1176–1181 (2012).

155. Oschmann, B. et al. Copolymerization of polythiophene and sulfur to improve the electrochemical performance in lithium–sulfur batteries. *Chem. Mater.* **27**, 7011–7017 (2015).

156. Li, L. et al. Molecular understanding of polyelectrolyte binders that actively regulate ion transport in sulfur cathodes. *Nat. Commun.* **8**, 2277 (2017).

157. Bucur, C. B., Muldoon, J. & Lita, A. A layer-by-layer supramolecular structure for a sulfur cathode. *Energy Environ. Sci.* **9**, 992–998 (2016).

158. Huang, J.-Q. et al. Ionic shield for polysulfides towards highly-stable lithium–sulfur batteries. *Energy Environ. Sci.* **7**, 347–353 (2014).

159. Kim, J. H., Choi, J., Seo, J., Kwon, J. & Paik, U. Two-dimensional Nafion nanoweb anion-shield for improved electrochemical performances of lithium–sulfur batteries. *J. Mater. Chem. A* **4**, 11203–11206 (2016).

160. Je, S. H. et al. Rational sulfur cathode design for lithium–sulfur batteries: sulfur-embedded benzoxazine polymers. *ACS Energy Lett.* **1**, 566–572 (2016).

161. Liu, J. et al. Molecularly imprinted polymer enables high-efficiency recognition and trapping lithium polysulfides for stable lithium sulfur battery. *Nano Lett.* **17**, 5064–5070 (2017).

162. Erk, C., Brezesinski, T., Sommer, H., Schneider, R. & Janek, J. Toward silicon anodes for next-generation lithium ion batteries: a comparative performance study of various polymer binders and silicon nanopowders. *ACS Appl. Mater. Interfaces* **5**, 7299–7307 (2013).

163. Lestriez, B., Bahri, S., Sandu, I., Roué, L. & Guyomard, D. On the binding mechanism of CMC in Si negative electrodes for Li-ion batteries. *Electrochem. Commun.* **9**, 2801–2806 (2007).

164. Bridel, J. S., Azaïs, T., Morcrette, M., Tarascon, J. M. & Larcher, D. Key parameters governing the reversibility of Si/Carbon/CMC electrodes for Li-ion batteries. *Chem. Mater.* **22**, 1229–1241 (2010).

165. Vogl, U. S. et al. Mechanism of interactions between CMC binder and Si single crystal facets. *Langmuir* **30**, 10299–10307 (2014).

166. Ryou, M.-H. et al. Mussel-inspired adhesive binders for high-performance silicon nanoparticle anodes in lithium-ion batteries. *Adv. Mater.* **25**, 1571–1576 (2013).

167. Jeong, Y. K. et al. Hyperbranched β-cyclodextrin polymer as an effective multidimensional binder for silicon anodes in lithium rechargeable batteries. *Nano Lett.* **14**, 864–870 (2014).

168. Jeong, Y. K., Kwon, T., Lee, I., Kim, T. S. & Coskun, A. Millipede-inspired structural design principle for high performance polysaccharide binders in silicon anodes. *Energy Environ. Sci.* **8**, 1224–1230 (2015).

169. Han, Z.-J. et al. High-capacity Si–graphite composite electrodes with a self-formed porous structure by a partially neutralized polyacrylate for Li-ion batteries. *Energy Environ. Sci.* **5**, 9014–9020 (2012).

170. Nguyen, C. C., Yoon, T., Seo, D. M., Guduru, P. & Lucht, B. L. Systematic investigation of binders for silicon anodes: interactions of binder with silicon particles and electrolytes and effects of binders on solid electrolyte interphase formation. *ACS Appl. Mater. Interfaces* **8**, 12211–12220 (2016).

171. Yao, Y., Liu, N., McDowell, M. T., Pasta, M. & Cui, Y. Improving the cycling stability of silicon nanowire

anodes with conducting polymer coatings. *Energy Environ. Sci.* **5**, 7927–7930 (2012).

172. Wu, H. et al. Stable Li-ion battery anodes by in-situ polymerization of conducting hydrogel to conformally coat silicon nanoparticles. *Nat. Commun.* **4**, 1943–1946 (2013).

173. Yu, X. et al. Three-dimensional conductive gel network as an effective binder for high-performance Si electrodes in lithium-ion batteries. *ACS Appl. Mater. Interfaces* **7**, 15961–15967 (2015).

174. Munaoka, T. et al. Ionically conductive self-healing binder for low cost Si microparticles anodes in Li-ion batteries. *Adv. Energy Mater.* **414**, 1703138 (2018).

175. Goodenough, J. B. & Kim, Y. Challenges for rechargeable Li batteries. *Chem. Mater.* **22**, 587–603 (2010).

176. Gauthier, M. et al. Electrode–electrolyte interface in Li-ion batteries: current understanding and new insights. *J. Phys. Chem. Lett.* **6**, 4653–4672 (2015).

177. Xu, K. Electrolytes and interphases in Li-ion batteries and beyond. *Chem. Rev.* **114**, 11503–11618 (2014).

178. Li, Y. et al. Atomic structure of sensitive battery materials and interfaces revealed by cryo-electron microscopy. *Science* **358**, 506–510 (2017).

179. Wang, X. et al. New insights on the structure of electrochemically deposited lithium metal and its solid electrolyte interphases via cryogenic TEM. *Nano Lett.* **17**, 7606–7612 (2017).

180. Zachman, M. J., Tu, Z., Choudhury, S., Archer, L. A. & Kourkoutis, L. F. Cryo-STEM mapping of solid–liquid interfaces and dendrites in lithium-metal batteries. *Nature* **560**, 345–349 (2018).

181. Jin, Y. et al. Identifying the structural basis for the increased stability of the solid electrolyte interphase formed on silicon with the additive fluoroethylene carbonate. *J. Am. Chem. Soc.* **139**, 14992–15004 (2017).

182. Michan, A. L. et al. Fluoroethylene carbonate and vinylene carbonate reduction: understanding lithium-ion battery electrolyte additives and solid electrolyte interphase formation. *Chem. Mater.* **28**, 8149–8159 (2016).

183. Aurbach, D. Review of selected electrode–solution interactions which determine the performance of Li and Li ion batteries. *J. Power Sources* **89**, 206–218 (2000).

184. Tang, Y. et al. Water-soluble sericin protein enabling stable solid-electrolyte interphase for fast charging high voltage battery electrode. *Adv. Mater.* **29**, 1701828 (2017).

185. Sun, B. et al. At the polymer electrolyte interfaces: the role of the polymer host in interphase layer formation in Li-batteries. *J. Mater. Chem. A* **3**, 13994–14000 (2015).

186. Xu, C. et al. Interface layer formation in solid polymer electrolyte lithium batteries: an XPS study. *J. Mater. Chem. A* **2**, 7256–7264 (2014).

187. Song, J., Lee, H., Choo, M.-J., Park, J.-K. & Kim, H.-T. Ionomer-liquid electrolyte hybrid ionic conductor for high cycling stability of lithium metal electrodes. *Sci. Rep.* **5**, 14458 (2015).

188. Tu, Z. et al. Designing artificial solid-electrolyte interphases for single-ion and high-efficiency transport in batteries. *Joule* **1**, 394–406 (2017).

189. Zhu, B. et al. Poly(dimethylsiloxane) thin film as a stable interfacial layer for high-performance lithium-metal battery anodes. *Adv. Mater.* **29**, 1603755 (2016).

190. Luo, J., Fang, C.-C. & Wu, N.-L. High polarity poly(vinylidene difluoride) thin coating for dendrite-free and high-performance lithium metal anodes. *Adv. Energy Mater.* **8**, 1701482 (2017).

191. Liu, Y. et al. An artificial solid electrolyte interphase with high Li-ion conductivity, mechanical strength, and flexibility for stable lithium metal anodes. *Adv. Mater.* **29**, 1605531 (2016).

192. Gao, Y. et al. Interfacial chemistry regulation via a skin-grafting strategy enables high-performance lithium-metal batteries. *J. Am. Chem. Soc.* **139**, 15288–15291 (2017).

193. Lopez, J. et al. Effects of polymer coatings on electrodeposited lithium metal. *J. Am. Chem. Soc.* **140**, 11735–11744 (2018).

194. Yang, H., Leow, W. R. & Chen, X. Thermal-responsive polymers for enhancing safety of electrochemical storage devices. *Adv. Mater.* **30**, 1704347 (2018).

195. Hu, W. The melting point of chain polymers. *J. Chem. Phys.* **113**, 3901–3908 (2000).

196. Orendorff, C. J., Lambert, T. N., Chavez, C. A., Bencomo, M. & Fenton, K. R. Polyester separators for lithium-ion cells: improving thermal stability and abuse tolerance. *Adv. Energy Mater.* **3**, 314–320 (2012).

197. Zhang, J. et al. Sustainable, heat-resistant and flame-retardant cellulose-based composite separator for high-performance lithium ion battery. *Sci. Rep.* **4**, 4419 (2014).

198. Lin, D., Zhuo, D., Liu, Y. & Cui, Y. All-integrated bifunctional separator for Li dendrite detection via novel solution synthesis of a thermostable polyimide separator. *J. Am. Chem. Soc.* **138**, 11044–11050 (2016).

199. Simha, R. & Boyer, R. F. On a general relation involving the glass temperature and coefficients of expansion of polymers. *J. Chem. Phys.* **37**, 1003–1007 (1962).

200. Hoffman, D. M. & McKinley, B. M. Crystallinity as a selection criterion for engineering properties of high density polyethylene. *Polym. Eng. Sci.* **25**, 562–569 (1985).

201. Chen, Z. et al. Fast and reversible thermoresponsive polymer switching materials for safer batteries. *Nat. Energy* **1**, 15009 (2016).

202. Kelly, J. C., Degrood, N. L. & Roberts, M. E. Li-ion battery shut-off at high temperature caused by polymer phase separation in responsive electrolytes. *Chem. Commun.* **51**, 5448–5451 (2015).

203. Shi, Y., Zhang, Q., Zhang, Y., Jia, L. & Xu, X. Promising and reversible electrolyte with thermal switching behavior for safer electrochemical storage devices. *ACS Appl. Mater. Interfaces* **10**, 7171–7179 (2018).

204. Scudamore, M. J., Briggs, P. J. & Prager, F. H. Cone calorimetry—a review of tests carried out on plastics for the association of plastic manufacturers in Europe. *Fire Mater.* **15**, 65–84 (1991).

205. Stalin, S., Choudhury, S., Zhang, K. & Archer, L. A. Multifunctional cross-linked polymeric membranes for safe, high-performance lithium batteries. *Chem. Mater.* **30**, 2058–2066 (2018).

206. Liu, K. et al. Electrospun core-shell microfiber separator with thermal-triggered flame-retardant properties for lithium-ion batteries. *Sci. Adv.* **3**, e1601978 (2017).

207. Zhou, G. et al. An aqueous inorganic polymer binder for high performance lithium–sulfur batteries with flame-retardant properties. *ACS Cent. Sci.* **4**, 260–267 (2018).

208. Trigg, E. B. et al. Self-assembled highly ordered acid layers in precisely sulfonated polyethylene produce efficient proton transport. *Nat. Mater.* **17**, 725–731 (2018).

209. Yanagisawa, Y., Nan, Y., Okuro, K. & Aida, T. Mechanically robust, readily repairable polymers via tailored noncovalent cross-linking. *Science* **359**, 72–76 (2018).

210. Filippidi, E. et al. Toughening elastomers using mussel-inspired iron-catechol complexes. *Science* **358**, 502–505 (2017).

211. Garcia, J. M. et al. Recyclable, strong thermosets and organogels via paraformaldehyde condensation with diamines. *Science* **344**, 732–735 (2014).

212. Lampel, A. et al. Polymeric peptide pigments with sequence-encoded properties. *Science* **356**, 1064–1068 (2017).

213. Fu, G. & Kyu, T. Effect of side-chain branching on enhancement of ionic conductivity and capacity retention of a solid copolymer electrolyte membrane. *Langmuir* **33**, 13973–13981 (2017).

214. Chintapalli, M. et al. Relationship between conductivity, ion diffusion, and transference number in perfluoropolyether electrolytes. *Macromolecules* **49**, 3508–3515 (2016).

215. Doeff, M. M., Edman, L., Sloop, S. E., Kerr, J. & De Jonghe, L. C. Transport properties of binary salt polymer electrolytes. *J. Power Sources* **89**, 227–231 (2000).

216. Ferry, A. Ionic interactions and transport properties in methyl terminated poly(propylene glycol)(4000) complexed with $LiCF_3SO_3$. *J. Phys. Chem. B* **101**, 150–157 (1997).

217. Chai, J. et al. In situ generation of poly (vinylene carbonate) based solid electrolyte with interfacial stability for $LiCoO_2$ lithium batteries. *Adv. Sci.* **4**, 1600377 (2016).

218. Tanaka, R., Fujita, T., Nishibayashi, H. & Saito, S. Ionic conduction in poly (ethylenimine)and poly (N-methylethylenimine)-lithium salt systems. *Solid State Ion.* **60**, 119–123 (1993).

219. Pehlivan, L. B., Gorën, P., Marsal, R., Granqvist, C. G. & Niklasson, G. A. Ion conduction of branched polyethyleneimine–lithium bis(trifluoromethylsulfonyl) imide electrolytes. *Electrochim. Acta* **57**, 201–206 (2011).

220. Ranger, M. & Leclerc, M. New base-doped polyfluorene derivatives. *Macromolecules* **32**, 3306–3313 (1999).

221. Sengodu, P. & Deshmukh, A. D. Conducting polymers and their inorganic composites for advanced Li-ion batteries: a review. *RSC Adv.* **5**, 42109–42130 (2015).

222. Shi, H., Liu, C., Jiang, Q. & Xu, J. Effective approaches to improve the electrical conductivity of PEDOT:PSS: a review. *Adv. Electron. Mater.* **1**, 1500017 (2015).

223. Zhang, X.-Q., Cheng, X.-B., Chen, X., Yan, C. & Zhang, Q. Fluoroethylene carbonate additives to render uniform Li deposits in lithium metal batteries. *Adv. Funct. Mater.* **27**, 1605989 (2017).